HIGH-RESOLUTION SEDIMENTARY RECORD IN A NEW BDP-99 CORE FROM POSOL'SK BANK IN LAKE BAIKAL

Baikal Drilling Project Group*

Another BDP drilling experiment was carried out in the winter of 1999 at 52°05′23″N—105°50′24″ E, under 201 m of water, on the slope of the Posol'sk Bank, a submerged bottom rise in South Baikal.

The ~350 m core spanning 1.2–1.3 myr is composed of alternating diatomaceous mud and glacial clays. Diatom stratigraphy and paleomagnetic data show a ca. 200 kyr deposition gap at 134 m, though the core contains the complete Brunhes chron of direct polarity (0–780 kyr). This unconformity, discovered for the first time in the Baikal cores, is direct evidence for tectonic activity in the Selenga region between 0.820 and 1.0 myr, during the uplift of the Primorsky Ridge inferred from land data.

The diatom record in the core correlates well with the marine oxygen isotope stratigraphy and indicates climate-driven variations in diatom production. High-resolution pollen records spanning an interval from 0 to 130 kyr provide a clue to climate change in the Baikal region and Transbaikalia.

Correlation of the BDP core and seismic profiling data allows age referencing of the seismoacoustic units and reflections which can be extrapolated onto a large area of the Posol'sk Bank and the shallow-water region near the Selenga Delta.

The obtained results shed light on the Pleistocene climate history in the region and the geological history of the Baikal rift.

Deep drilling, Lake Baikal, bottom sediments, lithology, sedimentation, seismic profiles, paleoclimate, paleomagnetism, deposition gap, diatom and pollen stratigraphy

INTRODUCTION

We report results of another BDP experiment in the winter of 1999 on the slope of the Posol'sk Bank, a submerged bottom rise on the southern termination of the Selenga-Buguldeika saddle separating the central and southern subbasins of Lake Baikal.

The first drilling on the Buguldeika Saddle (Leg I) [1, 2] was followed by experiments on the Academician Ridge in 1996 (Leg II) and 1998 (Leg IV) [3, 4] and in 1997 in the central Southern subbasin (Leg III) [5]. As a result, the deposition history was investigated in different geomorphic structures of Lake Baikal [6], gas hydrates were sampled for the first time in a freshwater lake [5], and a ~8 myr continuous paleoclimate record was obtained and is applicable for reference in climate reconstructions for Asia and the whole Northern hemisphere [3, 6–10]. The history of the Siberian climate recorded in the Baikal cores generally followed the global Earth's trend controlled by orbital insolation forcing [3, 4] but included climate events which are absent from the marine archives and represent the response of continental Eurasia to global climate change [10, 11]. A number of brief irregular excursions detected in the Baikal cores were independent of orbital forcing but caused by changes in the Northern Atlantic thermohaline circulation and in the regional atmospheric humidity (later Dryas and Bond cycles) [7, 8], which is evidence for a relationship between the Siberian and North Atlantic climate conditions. In general, the Baikal sediments store a record of the whole Cenozoic climate history of Central Asia.

*   E. Bezrukova, A. Bukharov, V. Bychinsky, S. Colman (USA), S. Fedenya, A. Gvozdkov, V. Geletii, A. Goreglyad, I. Gorokhov, E. Ivanov, T. Kawai (Japan), G. Kalmychkov, E. Karabanov, E. Kerber, B. Khakhaev, M. Khomutova, G. Khursevich, V. Kochukov, V. Kravchinsky, M. Krainov, S. Krapivina, N. Kudryashov, M. Kuz'min, N. Kulagina, P. Letunova, O. Levina, L. Pevzner, A. Prokopenko, C. Scholz (USA), P. Solotchin, L. Tkachenko, D. Williams (USA).

The drill site for the 1999 experiment (Leg V) was selected on the shallow-dipping slope of the Posol'sk Bank where a high-resolution record was expected due to high sedimentation rates and the absence of turbidites. The experiment on the Posol'sk Bank was planned to reach greater depths and provide a higher time resolution than the first BDP drilling at the Buguldeika Saddle in 1993 which was limited to a depth of 100 m and did not reach the Brunhes/Matuyama boundary.

The BDP-99 experiment started on 11 January 1999, on 22 January the drilling complex was frozen into position at 52°05′23″N—105°50′24″ E under 201 m of water. Drilling began on 28 January and ended on 8 March, together with geophysical logging. The team arrived at Port Baikal on 1 May. Continuous coring was completed to a depth of 350 m with a 95% core recovery to 255 m.

GEOLOGIC BACKGROUND

The BDP-99 experiment was run on the northwestern slope of the NE striking Posol'sk Bank in the South Baikal subbasin (Fig. 1), a 40 km long topographic high with its top under 35–55 m of water. It is a large half-horst with the southern part upthrown along a south dipping normal fault [12] which delineates the southern boundary of the bank consisting of several en-echelon normal faults dying out westward. The crystalline basement detected by multichannel seismic profiling at >3 km below the bank top (Fig. 2) [13] is overlain by a layered sedimentary sequence. Studies on manned submersibles on the steep southwestern slope of the bank revealed sedimentary rocks at depths of 910, 870, and 780 m [12] making up two regional-scale units: Lower Miocene silty sandstones and fine-grained sandstones cemented with carbonates at base are overlain by Middle-Upper Miocene gray cavernous dense carbonate-free clays composed of weathering products [14].

Seismic data. Multichannel seismic profiling images the sediments on the northwestern slope of the bank as an over 1000 m thick layered sequence (Fig. 2) [13, 15]. Continuous high-amplitude reflectors in the upper section indicate hemipelagic deposition in stable limnic conditions. The acoustic boundaries D4T and D3B (Fig. 2, line 92-8) [13] mark erosional unconformities, possibly caused by syndepositional changes in tectonic activity but are below the BDP-99 bore face. One more erosional unconformity (D2B), dated around 1.12 Ma [13], is above the hole face at ~190 m of subbottom depth. This surface is well pronounced in profiles across the Buguldeika Saddle and the Selenga shallow-water zone but is undetectable on the reflection profile 92-8 across the Posol'sk Bank (Fig. 2). The lower part of the slope is composed of chaotic blocks, apparently produced by landsliding, but the landslides are below the bore face.

Single-channel water-gun seismic reflection profiling (100–1060 Hz), with average sediment penetration of 300–400 m and a resolution of 1–2 m [16, 17], images a layered sedimentary sequence in the drill site (Fig. 3, *a*). The upper 220 m of sediments make up four acoustic units (line 92-67, Fig. 3, *b*). The upper unit, ~29 m thick and thickening upslope (Fig. 3), is marked by continuous reflectors much more prominent than in the other units. On the top of the bank, it lies unconformably and truncates the lower layers, and several unconformities occur in the lower section.

High-resolution (<0.5 m) seismic profiling using a 3.5 kHz system [16, 17] gave sediment penetration of 60 m. Lines 92-07 and 91-19 (Fig. 4) approach the bank's top. The sedimentary layers thin down towards the top and an erosional hiatus is well seen on the highest top part (Fig. 4, *b*). Therefore, seismic profiling indicates traces of erosion on the top of the bank and in the lower section but no evident signs of erosion immediately in the drill site.

Sedimentary sequence. Gravity coring of the upper slope of the Posol'sk Bank to a depth of 300 m shows diatom-bearing silty clay or clayey silt in the upper section underlain by thin dense glacial-lacustrine clays at depths of 0.9–1.5 m. The clays contain abundant 1–2 mm lenses of silt and fine-grained sand, possibly transported by ice and iceberg rafting [10, 18] and numerous thin (fractions of a millimeter) silt laminas likewise attributed to ice rafting. The oxidized surface layer on the slope is 1–2 cm thick.

Fine-grained modern deposits are absent only from the top, under 35 m of water, where glacial-lacustrine clays on the surface are overlain by 3–5 to 15–20 cm thick washed sand and gravel with numerous pebbles and small boulders. Gravel and pebbles are most often well rounded. Coarse-grained deposits are as a rule oxidized and cemented by ferromanganese crusts, especially abundant on the top of the bank (Karabanov, pers. commun.).

The lack of fine-grained modern deposits on the highest uplifted part of the bank attests to erosion by currents (confirmed by numerous traces of erosional microtopography on the clay surface) in the absence of modern deposition. Upper 10–20 cm of clays on the top, often oxidized and cemented by iron and manganese oxides, bear signature of long exposition and a long deposition gap. Pebbles and sand on the bank's top may have remained after fine-grained material had been washed out and evacuated by currents. Flat surfaces observed at water depths
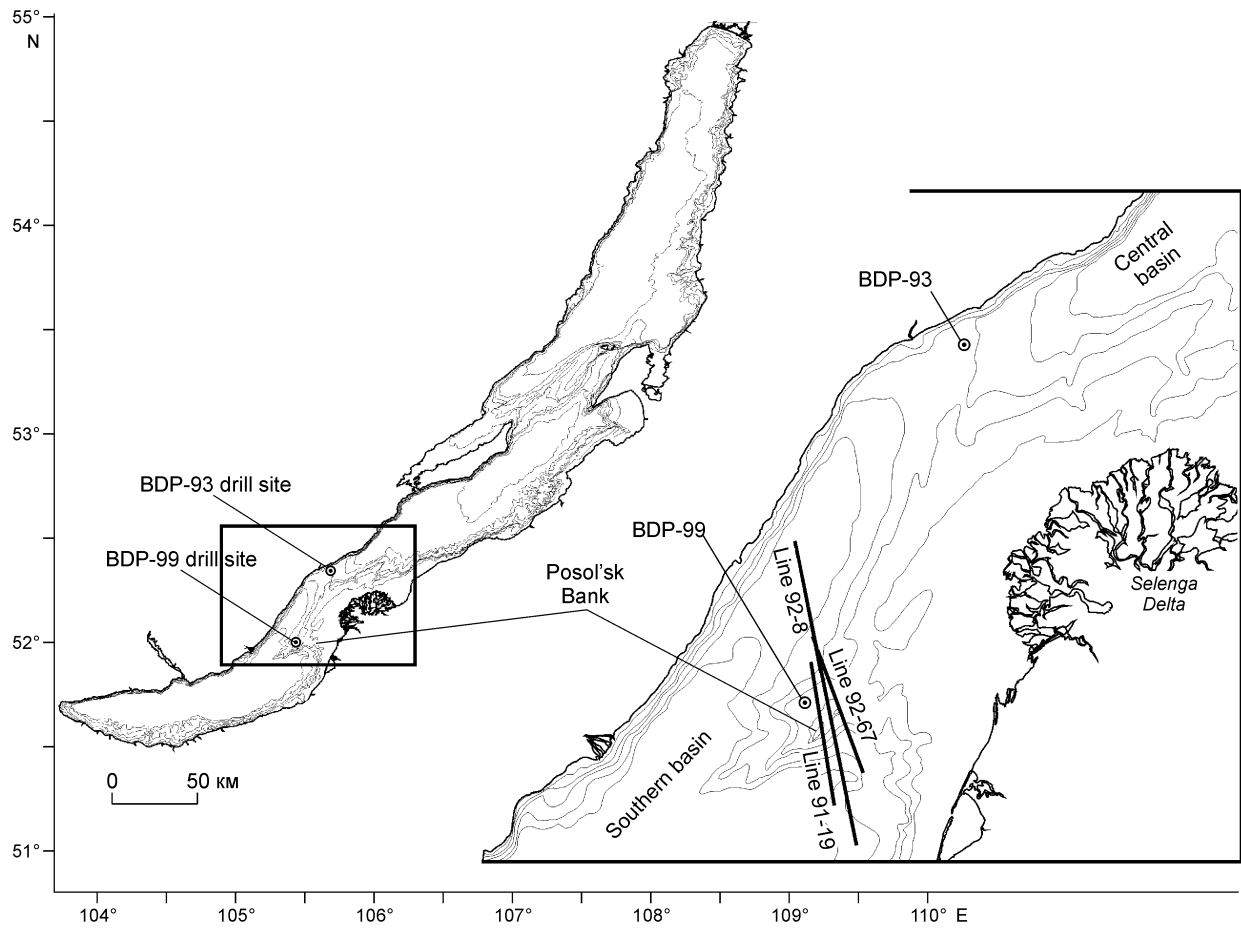
Fig. 1. Bathymetric map of Lake Baikal and BDP-99 core site location on Posol'sk Bank. Inset in right corner enlarges sampling area outlined by frame on map of Baikal and shows position of seismic reflection profiles (solid lines) from Figs. 2–4.
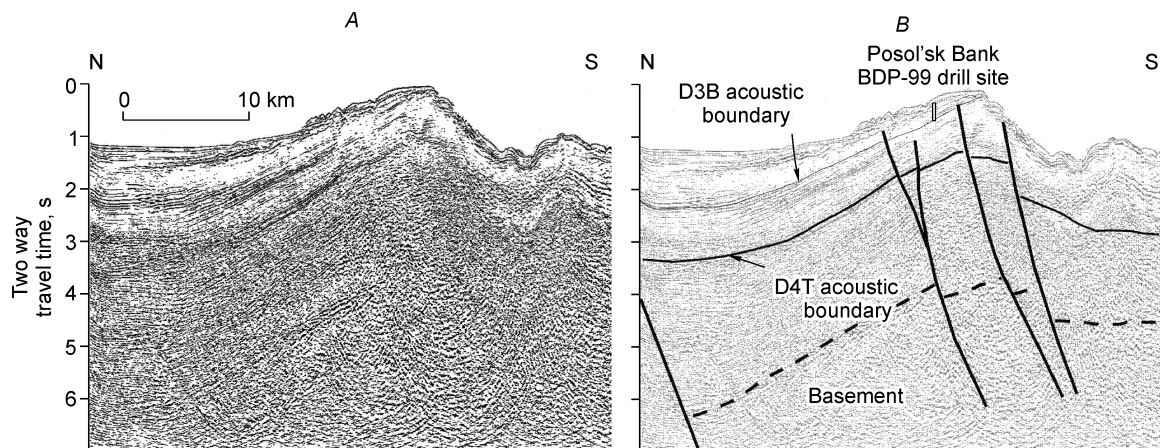
Fig. 2. Multichannel seismic profile 92-8 across the top of Posol'sk Bank (*A*) and its interpretation (*B*). Faults are shown as solid lines.
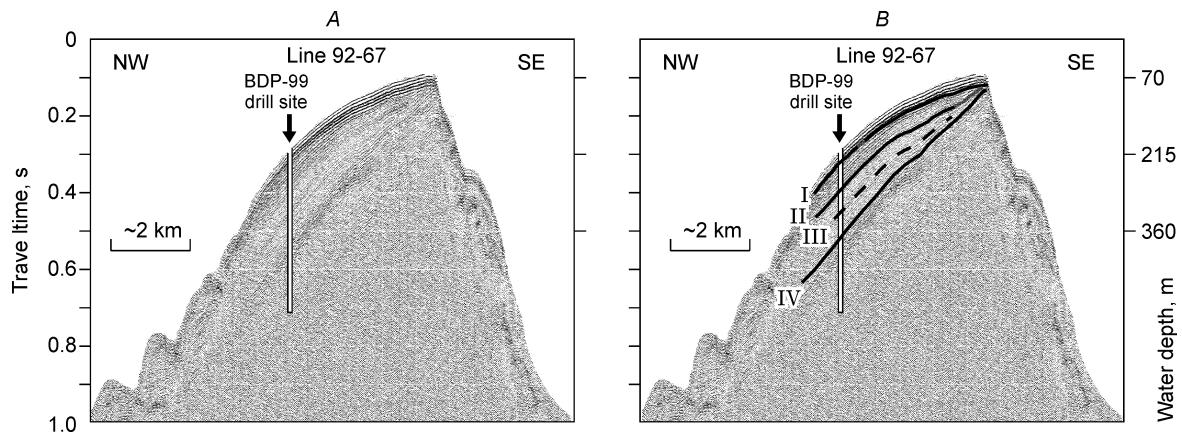
Fig. 3. Water-gun seismic reflection profile across the top of Posol'sk Bank. Arrow shows position and penetration of BDP-99 core. Profile 92-67 [16, 17] (*A*) and its interpretation (*B*). Roman numerals mark seismic units (see text).
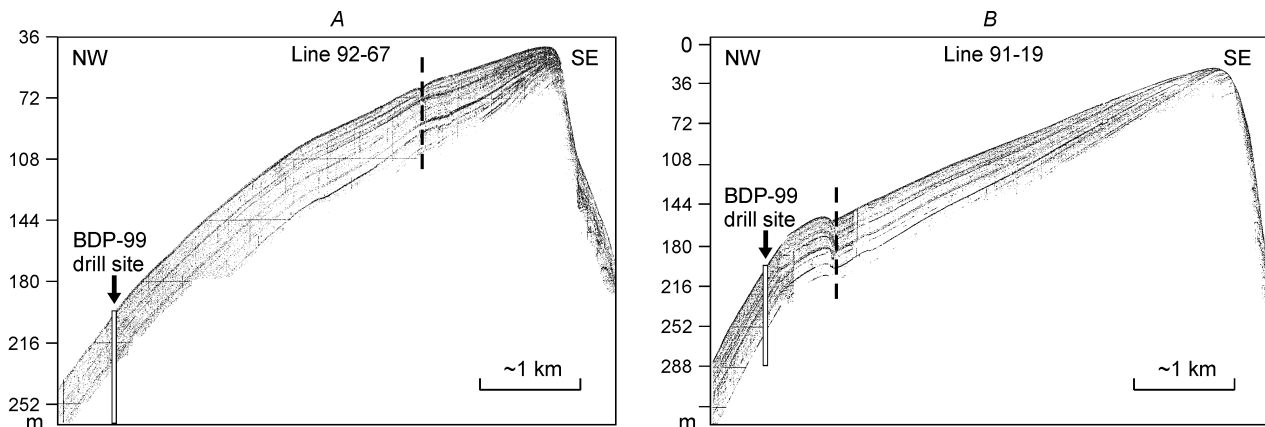
Fig. 4. High-resolution single-channel water-gun seismic profiles 92-67 (*A*) and 91-19 (*B*), after [16, 17]. Arrow shows position of BDP-99 core site.

of 35 and 50 m may be wave-cut terraces produced during a low stand, and pebbles and sand may be of beach origin.

Site selection. The BDP-99 drill site was selected on the shallow-dipping northwestern slope of the Posol'sk Bank in 200 m of water, far away from the top (Fig. 2); deeper drilling was unwise because of landslides detected in seismic profiles downslope below 300 m. Smooth topography, a well-pronounced Holocene section on the bank slopes, and the absence of acoustic boundaries (unconformities) indicated a long stable deposition and promised a continuous sedimentary record. High sedimentation rates were expected as the bank is located near the Selenga Delta on the way of river particulate fluxes [19, 20]. Therefore, according to preliminary seismic and geological evidence, the selected site was suitable for paleoclimatic studies. Drilling stripped a ~350 m section of undisturbed fine-grained layered sediments. Seismic profiling and acoustic velocity data [4] suggest that it did not reach the acoustic boundary D3B (Fig. 2) [13]. Thus, the core section was expected to be continuous prior to the experiment.

METHODS AND RESULTS

Drilling techniques. Two holes, 113 and 251.9 m deep, under 201 m of water, were drilled by the enhanced drilling system Nedra-Baikal-2000 mounted on a 1400 ton barge. The barge was trailed by the support ship "Baikal" and frozen into position at 52°05′21″N—105°50′21″E using satellite navigation.

The experiment was run in four stages. The drilling of the first hole began on 31 January 1999. The BDP-96 and BDP-98 experience demonstrated a risk of raiser breakup by ice shifting during freezing up in January-February when the ice-based drilling complex may move together with ice. The first hole, 0–113.27 m, was drilled without raiser in order to check the real section, to measure the depth of dense clays and to fix the raiser position. Drilling was interrupted after ten days, on 8 January, because of an ice shift. The second stage included raiser lowering and drilling of the second hole. The 245 mm raiser was lowered to the bottom and penetrated into the bottom sediments under 201 m of water to 218.78 and then 264.87 m of subbottom depth, and was not cemented. The second hole (0 to 251.9 m) was drilled from 10 to 21 February 1999. The third stage consisted in geophysical logging, and at the fourth stage an abandonment cement bridge was mounted between 40 and 50 m above the bottom and the raiser was lifted to the surface. The drill pipes (146 mm in diameter made of D16T alloy) were lowered and added under continuous depth control. Before lowering, the pipes were measured on rack by a steel tape to a precision of 0.001 m.

According to the project, the borehole had one-string casing. Coring was performed using the UKSB 178/56-79 Baikal-2 system with an advanced hydraulic piston corer (APC), a vibrocorer, and a rotary corer. This drilling rig was tested during the previous, BDP-93, BDP-96, BDP-97, and BDP-98, experiments. The BDP-99 holes were drilled using flushing with lake water (first hole) and with untreated bentonitic drilling mud (second hole).

The first hole was drilled to a total subbottom depth of 113.27 m and cored to 111 m with a core recovery of 98%. The second hole was drilled after the raiser was lowered to a total depth of 218.78 m (17.78 m of subbottom depth). Noncore drilling continued from 0 to 14 m, and the 14 to 109.27 m section was cored repeatedly to compensate for the core top loss in the first hole. Continuous piston coring between 109.27 and 151.88 m was completed by rotary coring from 151.88 to 251.9 m. The second hole was drilled to a total depth of 251.9 m and cored to 141.21 m with 98% recovery.

Drilling in the second hole to a depth of 350.5 m ran along with testing a new KUSK-185/56-79 Baikal Global corer which yielded 54.75 m of a conditioned core. The use of the new corer, when adjusted, is expected to cancel the drawbacks of the UKSB-178/56-79 corer and allow a deeper penetration and a higher rate of drilling with good quality and recovery of core.

The BDP-99 experience showed that it was reasonable to drill the pilot hole without raiser lowering during freezing up (January-February) to reduce the risk of ice shifting; the BDP-96, BDP-98, and BDP-99 experiments confirmed the necessity to control the position of the submerged string and the raiser to avoid their breakup by sudden ice shifts.

Lithology. The BDP-99 section is composed of fine-grained biogenic-terrigenous silty clay underlain by dense terrigenous silty clay, with minor amounts of sand-sized particles. See the distribution of the main lithological features in a composite cross section of the two holes in Fig. 5. The chart is based on semiquantitative counting in which the smear slide observation data by light microscope were compared with visual percentage charts [21, 22].

The BDP-99 section includes three lithologic units (Figs. 6, 7): the lower and intermediate units in the core BDP-99-2 and the upper unit in BDP-99-1. The lower unit, from 325 to 230 m subbottom depth, is composed of silty clay and minor sand (30 to 50% silt), often with partings of coarser material (over 20% of sand-sized particles). Gradational layering in some layers may indicate their turbidite origin. The section below 272 m is almost diatom-barren (Fig. 7).

The intermediate unit, from 230 to 120 m, is likewise made up of silty clay but has lower percentages of coarse material and higher diatom contents (locally up to 10–15%) than the underlying unit (Figs. 6, 7). Diatoms often occur as fragments or flow rings. The intermediate unit has a uniform composition. The percentage of silt (20–30%) is almost invariable, though the unit is over 100 m thick (Figs. 5, 6).

The upper unit of biogenic-terrigenous clay, from 0 to 120 m, has a more variable composition and percentages of the sand-silt fraction varying from 10 to 60% (Fig. 6). The upper 87 m has higher diatom contents than the lower unit (Fig. 7). Diatoms occur as full-size frustules and show a rhythmic distribution decreasing to zero or increasing to 20–40%. They are much less abundant and poorly preserved below 87 m though retain a cyclic distribution as far as the base of the unit (Fig. 7).

Diatom remnants coexist with sponge spicules (likewise composed of biogenic silica) throughout the BDP-99 section. The spicules are unevenly distributed and most often occur as fragments unlike the BDP-96 and BDP-98 cores where they were mostly intact [3, 4]. Spicules counted in smear slides vary in number from 0 to 10 and are most often attributed to diatom-rich layers.

The sediments have gray to olive-black reduced colors, as in the Academician Ridge and Buguldeika cores [1–4], and keep these colors as far as the section base. Therefore, the entire section was deposited in reducing conditions, under the water, and was never exposed above the lake surface. The darker shades of the BDP-99 sediments than in those from the Academician Ridge [3, 4] indicate higher contents of terrigenous material and
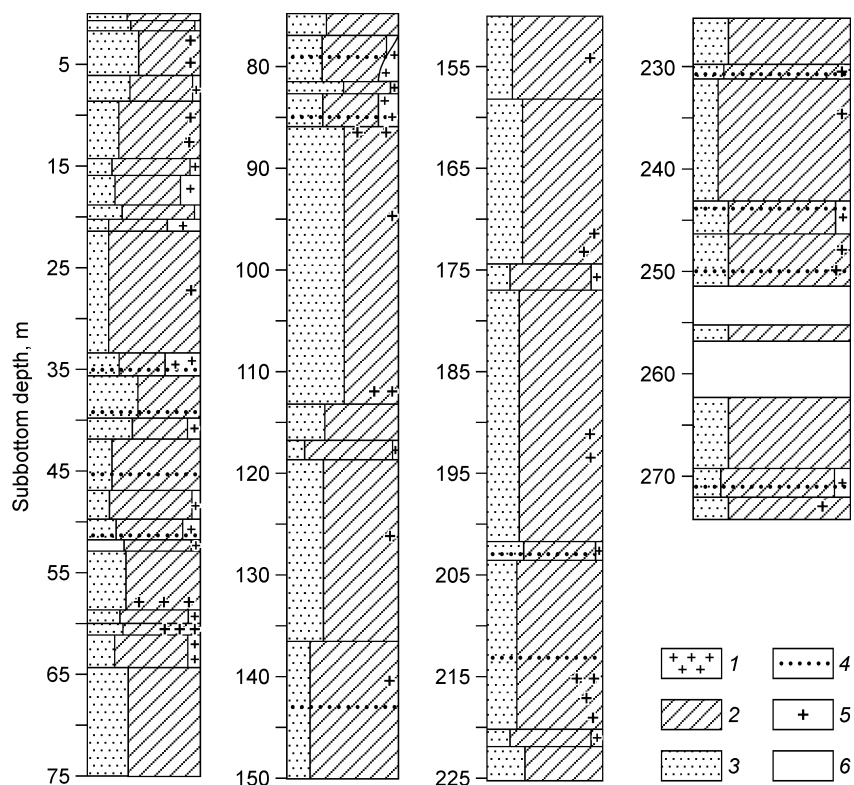
Fig. 5. Composite lithological profile of twin drill holes BDP-99-1 and BDP-99-2. *1* — diatoms; *2, 3* — clay- (*2*) and silt-sand-sized (*3*) particles; (*1–3* show proportions of components in vol.%); *4* — diatom contents less than 3%; *5* — sand and turbidite beds; *6* — missing core sections. Digits on the left refer to subbottom depths, in m.

organic carbon. Unlike the previous cores, the diatom-rich layers in the BDP-99 core are almost of the same color as the diatom-barren clay.

The BDP-99-2 core contains a 5.5 cm thick uppermost oxidized layer (which is rare for the sediments in the Selenga delta), and thus has been cored completely unlike BDP-99-1 missing the top section. The core top loss was 14–16 cm, estimated from core-to-core correlation against the indicator layer rich in *Synedra acus* var. *radians* diatoms ubiquitous in offshore Baikal [18], which is at 29.5–31 cm in BDP-99-1 and at 45.5–47 cm in BDP-99-2 (Fig. 8).

The textures are as a rule laminated, finely laminated, massive, or lenticular, made up by alternating diatom-rich and clay layers in the upper section and grain size variations. Fine lamination is weakly pronounced unlike that in the Academician Ridge cores. Few separate layers, within 5 cm thick, with fuzzy boundaries, bear coarse silt and fine sand particles and are unevenly distributed in the section, most often within the clay layers (Figs. 5, 6). High percentages of coarse sediments may be due to ice rafting.

Although the drill site is located on a submerged slope, the BDP-99 section is poor in turbidites. Several turbidite beds are restricted to the lower core at 349–350 m (Figs. 5, 6); a well-pronounced 19 cm thick turbidite occurs at 92.5 m in BDP-99-2 and its eroded base is composed of sand grading into silty and then into clay.

Traces of bioturbation are rare and irregular, especially rare in the lower section. Bioturbation in diatom layers is marked by small horizontal lenses slightly different in color from the surrounding sediments. Bioturbated clay is cut by thin crooked vertical or inclined channels from 1–2 to 7 cm long, often with vivianite inclusions, which disturb the layering and stand out in their color. Generally, traces of bioturbation are less prominent in the BDP-99 section than on the Academician Ridge.

Abundant lenticular textures not related to bioturbation are produced by small (fractions of a millimeter to a few centimeters) sand-silt lenses, most often in the upper 80 m of the section (Fig. 9) and mostly in clay layers (25–30 lenses per 1 m of the core surface). Thin sand lenses at depths of 19–20 m in diatomaceous mud, apparently
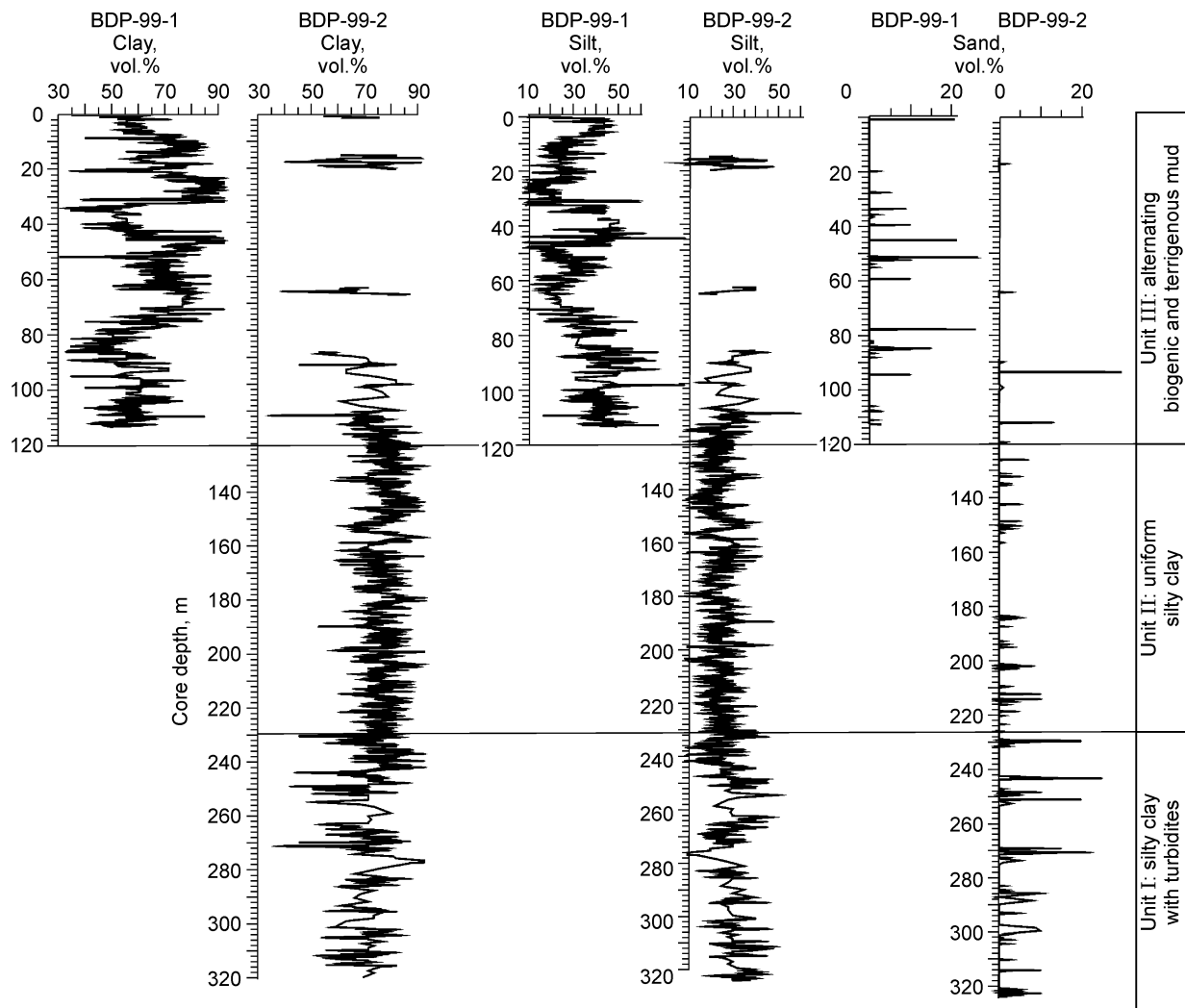
Fig. 6. Depth-dependent variations of clay-, silt- and sand-sized particles in BDP-99-1 and BDP-99-2. Column on the right shows lithological stratigraphy of sediments.

produced by ice rafting [3, 4, 10, 18], mark transitions to clay layers. Sand grains in the lenses are angular to subrounded.

Pebbles and gravel are encountered as scarce inclusions throughout the section (Fig. 10), almost always in clay, and are normally angular or poorly rounded quartz detritus or, less often, clasts of siltstones, schists, and granites. Plant remnants are very rare and are represented by coaly herb or wood fragments.

The cores contain abundant vivianite nodules, typical of the Baikal sediments [4, 29], often attributed to separate partings, mostly in the upper 50 m of the section; individual granules or segregations and aggregates occur throughout the section. The nodules are mostly small (2–5 mm, less often up to 1 cm) pockets of irregular shapes, composed of gray powdery material. Vivianite becomes oxidized and changes its color to bright blue in the air on core retrieval, which makes it easily detectable. Vivianite inclusions often occur along channels produced by benthic organisms and are much more abundant in the upper 65 m than in the lower section (Fig. 10).

The section also contains numerous bands, patches, mottles, and pockets of hydrotroillite (FeS·nH$_2$O), black powdery material turning into ocher-red when oxidized in the air. The BDP-99 section is richer in hydrotroillite than the cores from the Academiciain Ridge.

Physical properties of bottom sediments. The density of sediments in the depth interval from 180 to 350 m was measured by weighing about 400 mg specimens of as-dredged core on torsion balance in the air and in kerosene. The mean density of the sediments is 1.97 g/cm^3 (from 1.84 to 2.10 g/cm^3), lower in diatom-bearing layers and higher in diatom-barren clay. The density variations are consistent with diatom and water content
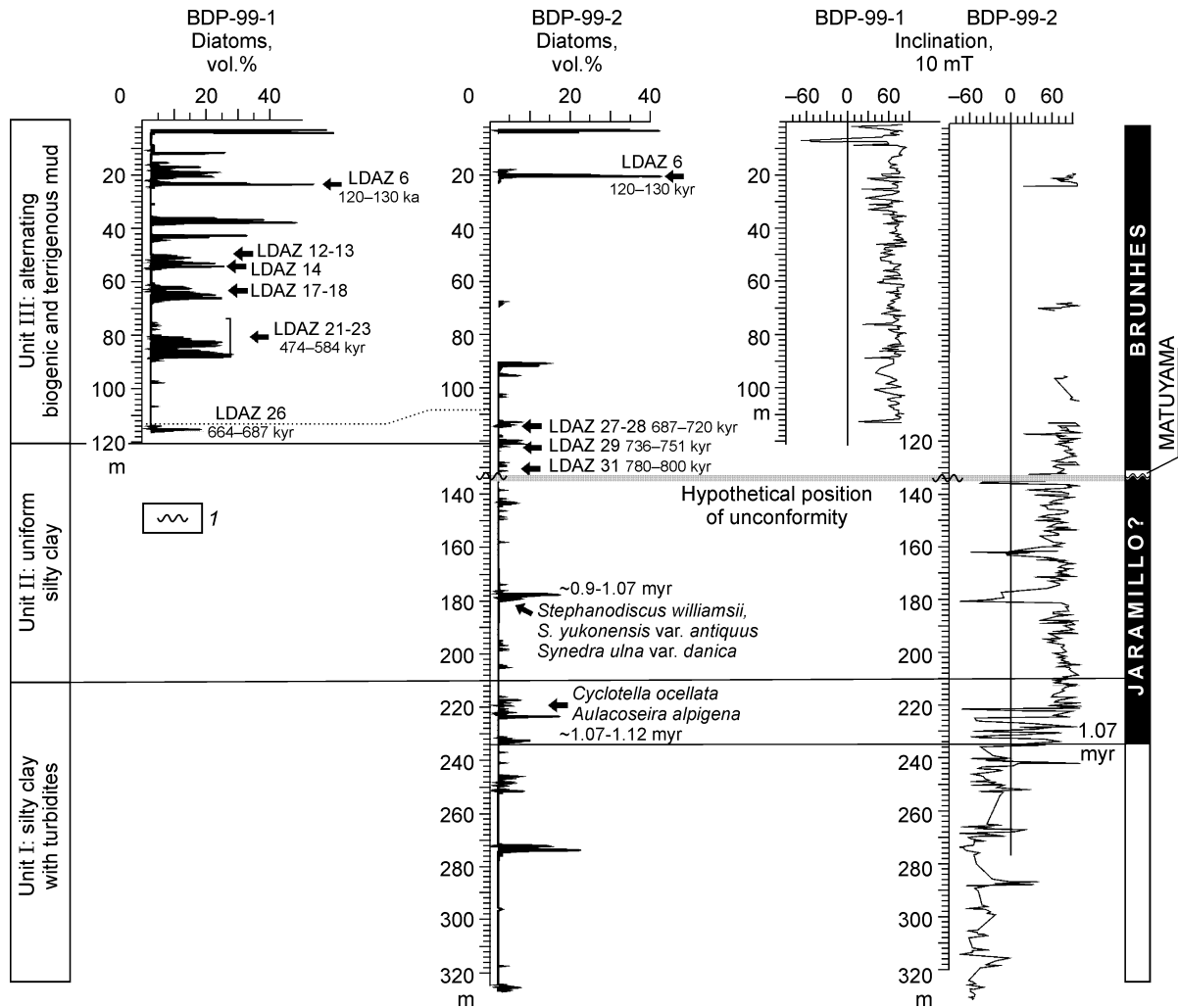
Fig. 7. Diatom and magnetic stratigraphy of twin drill holes BDP-99-1 and BDP-99-2. Column on the left shows lithological stratigraphy of sediments. Diatom abundances are given for two holes. Arrows show local diatom zones (LDAZ) in BDP-96 [26]. On the right are inclination profiles and possible interpretation of the available data according to the magnetostratigraphic scale. *1* **— hypothetical unconformity.**

variations. Density generally increases downcore with gravity compaction. The sediments of the Posol'sk Bank are denser than in the Academician Ridge because of higher percentages of the terrigenous component.

The water content was measured immediately after dredging the core. Specimens about 1 cm^3 sampled at every 10 cm were weighed, dried at 60 °C, and reweighed. Water contents in 2079 analyzed samples range from 18.9 to 64.6% and decrease regularly down the section (Fig. 11) because of gravity compaction to 19–22% at the bore face. A similar decrease in water content associated with gravity compaction was observed in the BDP-93 core [1], better pronounced there than on the Academician Ridge [3, 4].

Generally decreasing downcore, the water contents vary strongly depending on lithology and, especially, on diatom percentage. Comparison of water and diatom content curves (Fig. 11) shows that diatom-rich layers as a rule have higher water contents than clays, and this proportion holds throughout the section. Water content changes on transition from diatomaceous mud to clay were likewise noted in the Buguldeika and Academician Ridge cores [1–4] and were thus suggested as a simplified lithological and climate proxy [23, 24].

Geophysical logging (Table 1) included measurements of resistance (RL), resistivity (RTL), self-potential (SPL), gamma radioactivity (GL), acoustic waves (AL), low-field whole-core magnetic susceptibility (KL), induction (IL), cement ring (CRL), temperature (TM), and inclination (ICL). Gamma radioactivity was measured in open hole and in the raiser.

Table 1

Method	RL	SPL	GL*	KL	AL	IL	RTL	TM*	ICL*
Core depths BDP-99 (m)	63–178	63–183	0–274	63–171	63–176	63–169	0–185	0–260	16–182

* Measurements were taken in hole and in water column; other measurements were taken in hole in bottom sediments.

Temperature measurements allowed estimates of the geothermal gradient and temperatures of sediments (17.8 mK/m and 4.6–7.9 °C, respectively) at depths between 0 and 185 m (Table 2).

Paleomagnetic studies. Low-field whole-core magnetic susceptibility (K) of the BDP-99 cores was measured at every 20 cm in 1223 samples. It is inversely proportional to diatom contents, especially in the upper 87 m, as in the previously studied Baikal cores [3, 4]. However, correlation of the K record with the marine oxygen isotope stratigraphy is more difficult in BDP-99 (even in the upper section) than in the cores from the Academican Ridge [3, 4]. The magnetic susceptibility curve in the intermediate BDP-99 unit indicates a uniform lithology (Fig. 12).

Inclination was measured in 656 samples from both holes, 602 samples from core end surfaces and 54 samples from core halves split for detailed demagnetization. All samples were demagnetized in a stepwise alternating field (AF) at the Paleomagnetic Laboratory (Irkutsk) and then measured on a JR-4 magnetometer (Czech Republic).
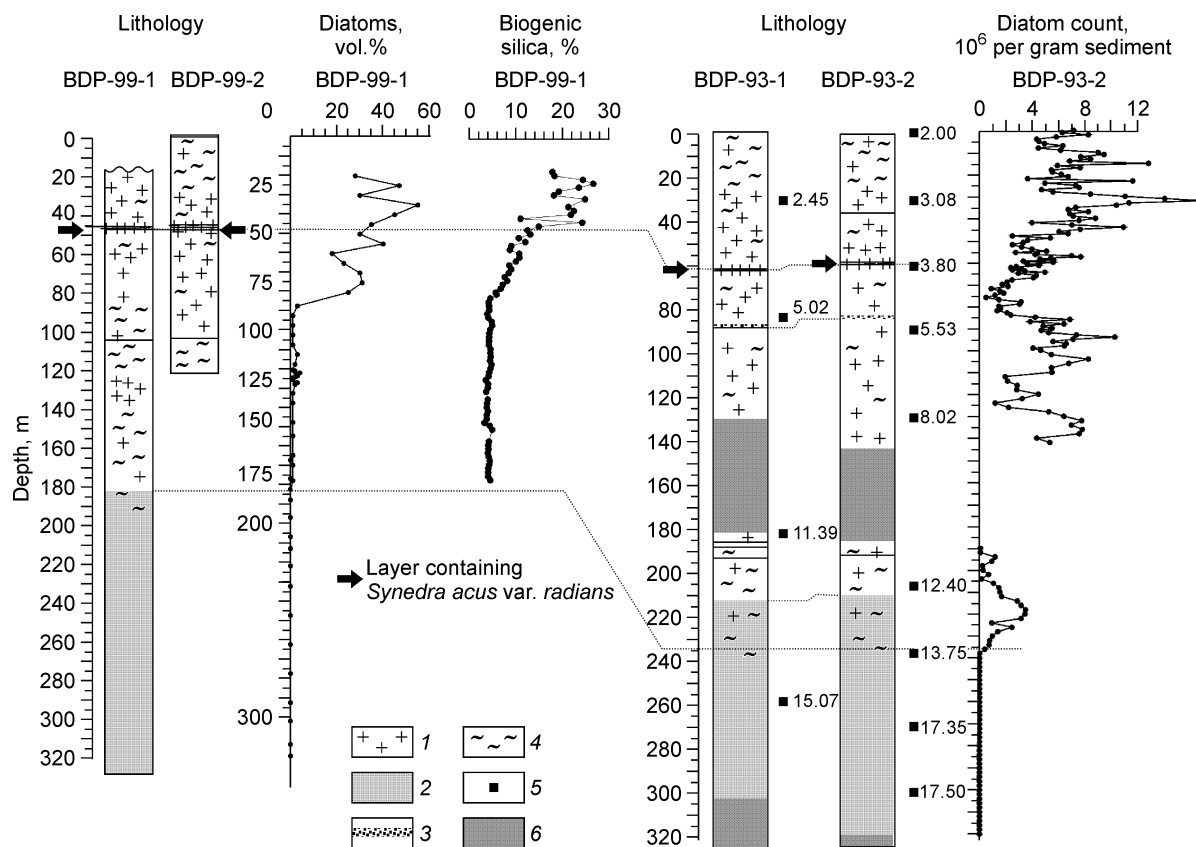
Fig. 8. Lithology and correlation of BDP-99-1 and BDP-99-2 (on the left); depth-dependent variations of diatom abundances and biogenic silica in BDP-99-1 (in the middle); lithology and correlation of BDP-93-1 and BDP-93-2 (Buguldeika Saddle); diatom abundances in BDP-93-2 (on the right). Black squares mark position and AMS ^{14}C ages (kyr) [29]. Arrows show position of thin 3.8 kyr [74] layer of *Synedra acus* chosen for reference in correlation of BDP-99 and BDP-93. *1* — diatoms, *2* — silty clay, *3* — turbidite, *4* — terrigenous mud, *5* — AMS ^{14}C ages, *6* — missing core sections.
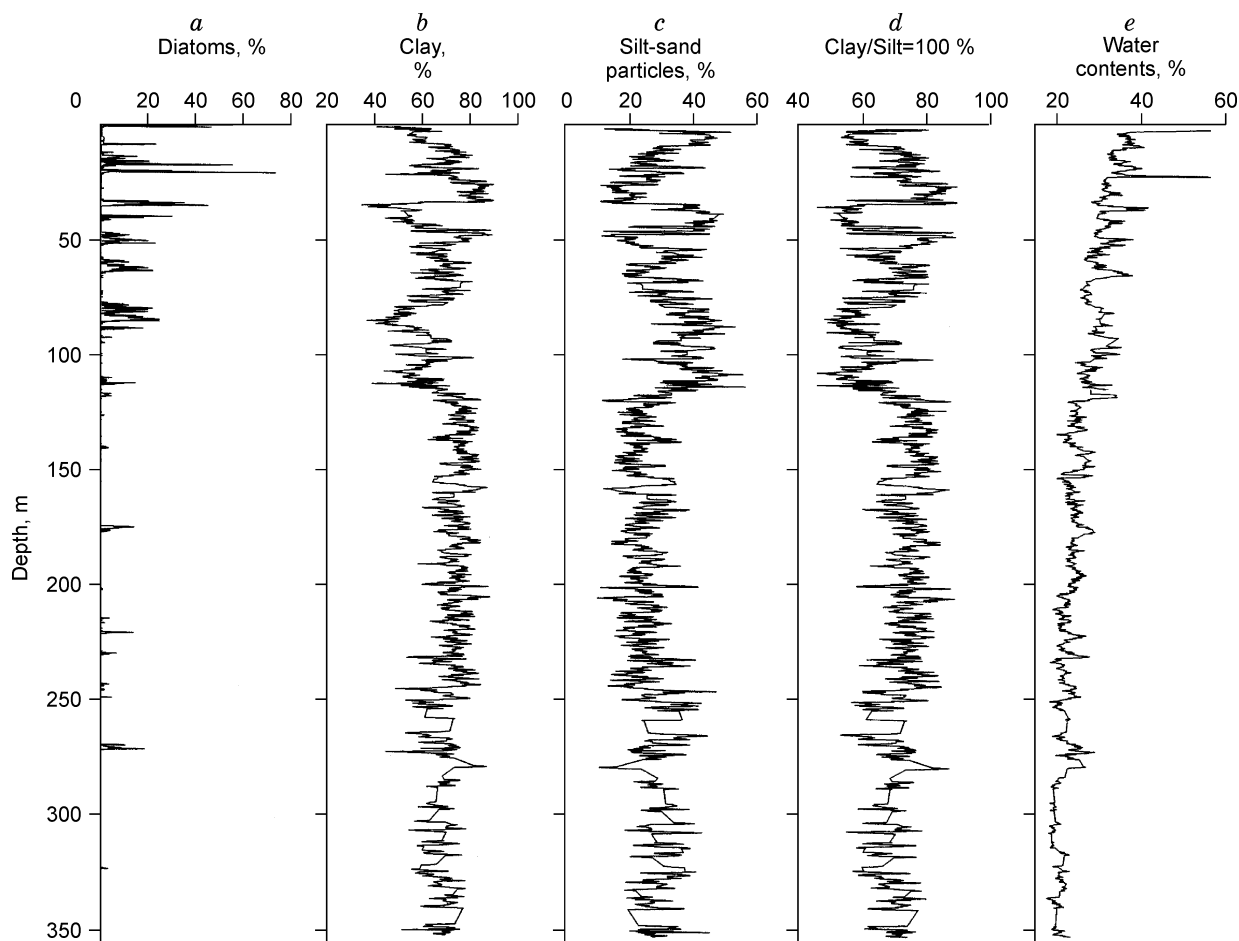
Fig. 9. Depth-dependent variations of lithology and physical properties of sediments. *a* — diatoms; *b* — clay; *c* — silt-sand-sized particles; *d* — proportion of clay and sand-silt-sized particles, normalized to 100 %; *e* — water content (average over four points).

Table 2

Subbottom depth interval (m)	Temperature (°C)	Average geothermal gradient, mK/m
0–185	4.6–7.9	17.8

The paleomagnetic studies aimed at dating the section by correlation of the obtained remanence record with the reference magnetic time scale for the Cenozoic [25].

It was shown earlier [3, 4] that the viscous remanence component in the Baikal sediments produced by modern remagnetization overprints can be removed in a 10 mT field, which was confirmed by the detailed demagnetization of 54 BDP-99 samples. Therefore, the other samples were demagnetized at 5, 10, and 20 mT.

The NRM record of AF demagnetized samples from the two holes is shown in Fig. 7. If the change from direct to reverse polarity at 220–240 m is the Brunhes/Matuyama boundary (780 kyr), the following polarity change (Matuyama/Jaramillo, 990 kyr) can be expected at ~290 m, assuming an invariable sedimentation rate and the transition from Jaramillo back to Matuyama (1070 kyr) at 315 m, according to the reference magnetic time scale [25]. However, the BDP-99 paleomagnetic record does not show these polarity changes, and the section below 230 m was apparently deposited during a direct polarity episode, most likely the Jaramillo. Then the section misses the sediments deposited in the upper Matuyama Chron, i.e, ~150–200 m of the deposits may have been washed out and the sediments deposited during two episodes of direct polarity (Brunhes and Jaramillo) were brought
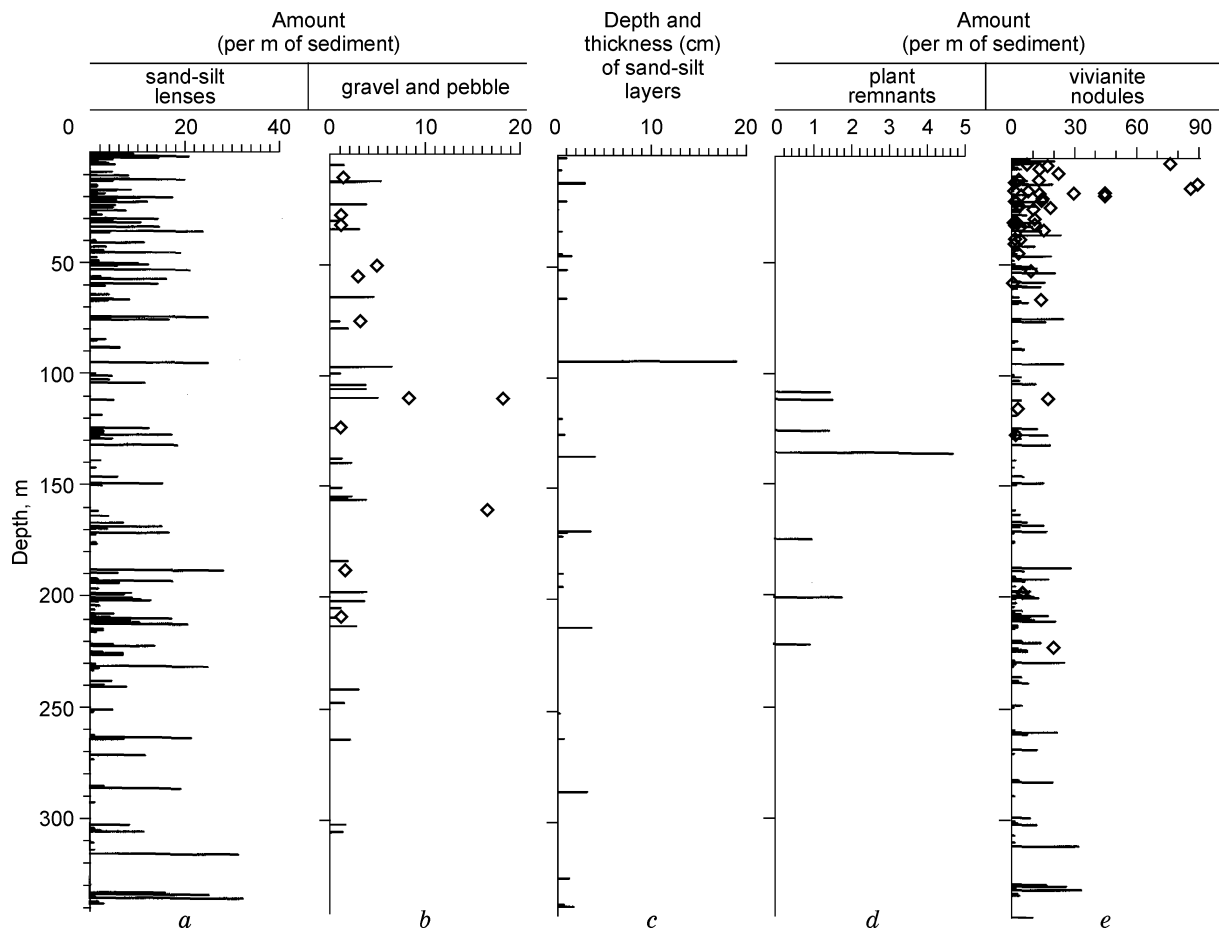
Fig. 10. Depth-dependent distribution of: *a* — sand and silt lenses; *b* — gravel and pebbles (rhombs); *c* — position and thickness (cm) of sand and silt layers; *d* — plant remnants; *e* — vivianite nodules (rhombs) in BDP-99-1 and BDP-99-2.

together. Thus paleomagnetic data alone cannot constrain the Brunhes and Jaramillo boundaries, but the position of the hiatus and the Brunhes/Matuyama transition can be determined using diatom stratigraphy.

DISTRIBUTION OF DIATOM CONTENTS IN BDP-99 SECTION

The diatom contents in BDP-99 were determined by semiquantitative counting along with distribution of terrigenous fractions [3, 4, 21, 22]. The obtained diatom records from the Posol'sk Bank, especially from the upper 80 m, demonstrate a typical rhythmic alternation of diatom-rich and diatom-barren layers formed in interglacial and glacial times, respectively (Fig. 7, 11). The mean diatom content decreases downcore, especially below 87 m (Fig. 7). The diatom percentages are the highest in the uppermost 0–1 m where they reach 47 vol.% (Figs. 7, 8). In the lower section, their concentration is 5–15% in some layers but most sediments are diatom-barren (Figs. 5–7). The diatoms in the BDP-99 cores are of rather poor preservation, many frustules occur as fragments or flow rings. For instance, *Cyclotella* rarely preserves its rims, possibly because of partial dissolution.

Preliminary diatom stratigraphy of BDP-99. The species composition of diatoms in the BDP-99 core, an important stratigraphic marker, was analyzed in samples from diatom-rich layers. The BDP-99 species composition was compared with the high-resolution biostratigraphic record of the BDP-96-2 core [26, 27] and was used in age modeling of BDP-99.

Section 1-1A (0–0.67 m) contains typical Baikal Holocene diatom assemblages: *Cyclotella minuta, C. ornata, Aulacoseira baicalensis, A. islandica* (spores), and *Stephanodiscus binderanus*. The section also contains a layer bearing *Synedra acus* var. *radians* similar to that found in the BDP-93 core [28] (Fig. 8) and elsewhere in the lake [18]. The AMS ^{14}C age of this diatom-bearing layer is 3.8 kyr [7, 28, 29].
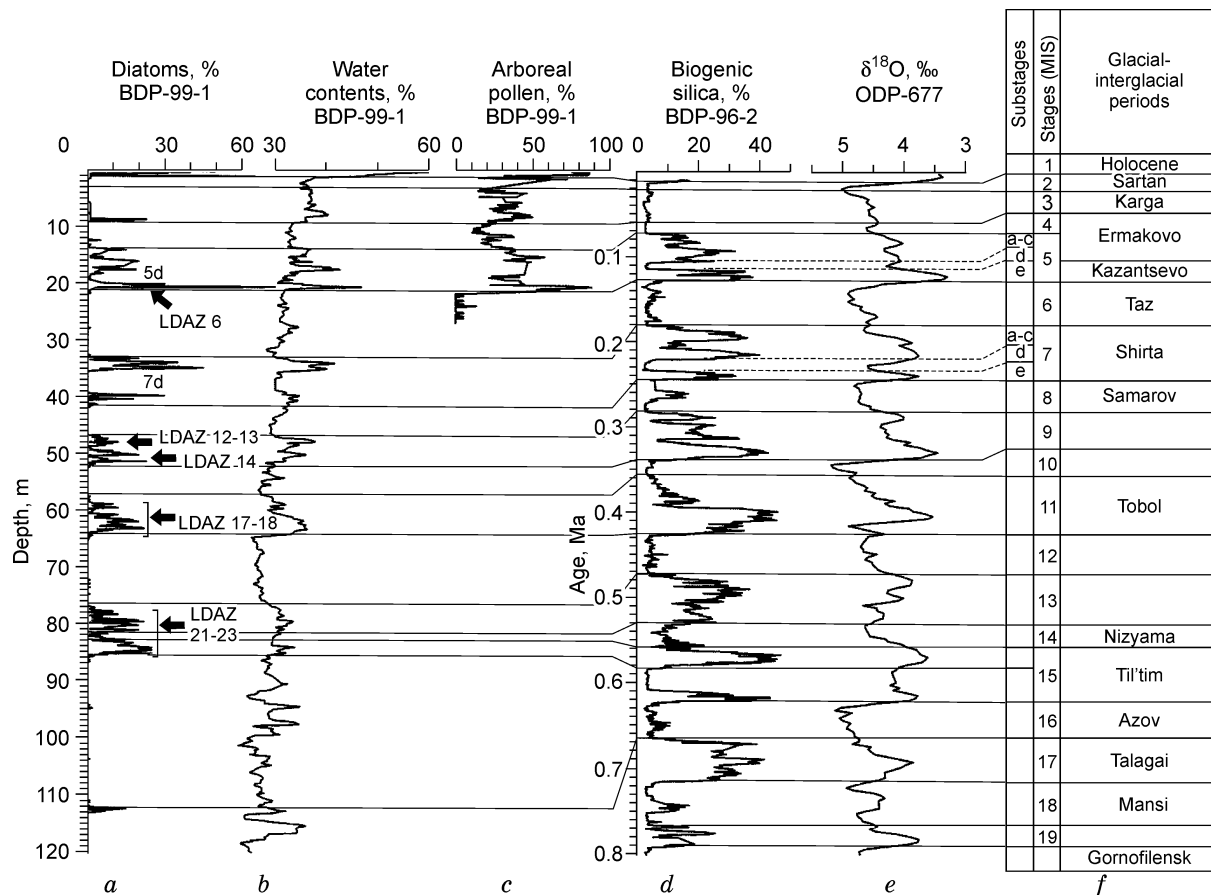
Fig. 11. Diatom abundances (*a*), water contents (*b*), and percentages of arboreal pollen (*c*) in BDP-99 core correlated with biogenic silica record of BDP-96-2 [52] (*d*) and ODP-677 marine oxygen isotope stratigraphy [50] (*e*). Column on the right (*f*) shows BDP-99-1 record compared to MIS stratigraphy and glacial-interglacial stratigraphy for West Siberia [53, 54].

The diatom abundance in a sample from section 5-1B (BDP-99-1) is much lower and the assemblage includes *Cyclotella minuta*, *C. ornata*, and *S. flabellatus* which record the Karga interstadial (Khursevich, pers. commun.). Section 14-1 (19.34–20.63 m) in BDP-99-1 contains species *Stephanodiscus grandis*, *S. formosus*, *S. carconeiformis*, *Synedra ulna* var. *dancia*, *Aulacoseira islandica* (frustules and spores). This assemblage is typical of the local diatom zone (LDAZ) 6 [26, 30] (Fig. 7), with the age corresponding to the last interglacial (Kazantsevo time) equivalent to MIS 5e (Fig. 11). The MIS 5e diatom assemblage in BDP-99 includes *Aulacoseira italica*, unlike the BDP-93 and BDP-96 cores.

A number of indicator species was also found downsection, such as the assemblage in section 21-23 (32.37–38.61 m) with *Stephanodiscus grandis*, *S. formosus*, *S. carconeiformis* typical of MIS 7 in BDP-99-2 [26, 30]. Section 30-31 (47.21–50.43 m) bearing *Stephanodiscus grandis* diatoms and abundant spores of *Aulacoseira islandica* may correspond to LDAZ 12-13 (MIS 9) [26, 30]. This correlation is confirmed by the presence of a specific LDAZ 14 assemblage corresponding to MIS 9 in section 32-1 (50.43–51.25 m) of BDP-99-1: abundance of *Stephanodiscus exiguus* and the occurrence of *S. baicalensis* var. *concinnis* [26, 30]. Section 38-1 (61.96–62.71 m) contains a Baikalian assemblage typical of the interglacial correlated with MIS 11. Like BDP-96-2, the BDP-99-1 cores of this interval bear *S. distinctus*, *S. exiguus*, *S. binderanus*, *Cyclotella minuta* and spores of *Aulacoseira islandica* (LDAZ 17-18 according to [26, 30]). The diatom assemblage from section 48-49 (76.68–79.03 m) in BDP-99-1 is dominated by *S. distinctus* et var. *excentricoides*. This interval corresponds to LDAZ 21 in BDP-96-2 correlated to MIS 13. Note that this diatom zone in BDP-99-1 contains *Cyclotella minuta*. The assemblage of section 51 (82.24–83.21 m) in BDP-99-1 is represented by a single species *S. distinctus* and has high contents of benthic diatoms, a combination distinctive of LDAZ 23 in BDP-96-2 [26, 30]. The diatom assemblage in section 70 (112.14–113.41 m) was the last age indicator found in BDP-99-1. The presence of
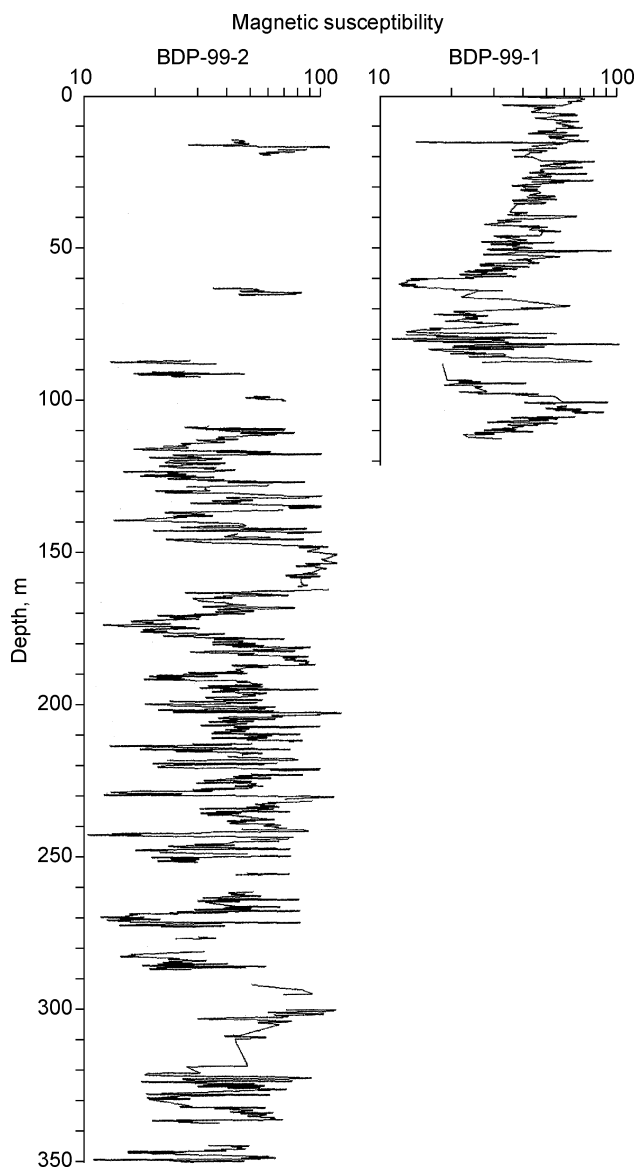
**Fig. 12. Low-field whole-core magnetic susceptibility pro-
files (K = 10³ SI units) for BDP-99-1 and BDP-99-2 cores.**

Cyclotella praeminuta and *Stephanodiscus baicalensis* var. *concinnis* allows us to correlate the interval with LDAZ 26 in BDP-96-2. Therefore, this interval at base of the upper unit of BDP-99 corresponds to MIS 17, about 664–687 kyr [26, 30].

It was difficult to find indicator species in the intermediate unit where diatoms are of poor preservation and lower contents. A representative sample was found in section 101 (227.07–229.01 m) in BDP-99-2 (Fig. 7) in which the diatom assemblage includes *Cyclotella ocellata* and *Aulacoseira alpigena*. A diatom assemblage dominated by *Cyclotella ocellata* was found earlier in BDP-96-2 between 47.6 and 49.6 m which corresponds to ~1.07−1.12 myr [31]. Therefore, the *Cyclotella ocellata* zone is an important stratigraphic marker for BDP-99. This interval in BDP-99 contains abundant *Aulacoseira alpigena*, whereas the same interval in BDP-96-2 contained *Aulacoseira subarctica* as the second dominant species [31]. The difference, however, does not contradict the correlation between BDP-96 and BDP-99, as both *A. alpigena* and *A. subarctica* are psychrophilic species. This cold interval with a typical diatom assemblage in the BDP-96 core was correlated to the Menap cold episode in Western Europe [31]. The assemblage of *Stephanodiscus williamsii*, *S. yukonensis* var. *antiquus* [31] and *Synedra ulna* var. *danica* is another significant marker in BDP-99-2. In section 57-58 (174.93–176.67 m) in BDP-99-2

(Fig. 7) it corresponds to the 0.9–1.07 myr assemblage in BDP-96-2 where it is above the *Cyclotella ocellata* Zone [31]. Therefore, Lower Pleistocene diatom assemblages in the BDP-99-2 section from the Posol'sk Bank show the same stratigraphy as in the Academician Ridge cores.

Spore-pollen stratigraphy. *Methods*. The upper 25 m of core section 1-17 were sampled at every 10 cm in order to obtain high-resolution vegetation records from the region of high sedimentation rates. The BDP-93 section deposited at a similar rate was sampled at every 40 cm throughout the 100 m whole-core length, and the BDP-96 section sampled at a 10 cm resolution was deposited in more stable conditions. Therefore, it was decided to sample the BDP-99 section at 10 cm to investigate its upper part which has the most important climate implications for the past millennia.

The samples were prepared for microscopic examination following the standard procedure [32]. The total of the counted pollen and spores varied from 5 to 2300 grains. Taxa percentages in the spore-pollen spectra (SPS) were determined only in samples where the spore and pollen sum exceeded 200 grains. Abundances or percentages of pollen taxa were estimated from total arboreal pollen. Altogether, we determined about 70 plants but the presented simplified percentage diagram is reduced to 17 elements.

Pollen stratigraphy. The pollen percentage record was divided into eleven assemblage zones (Fig. 13) on the basis of visually examined spore and pollen contents in the spectra and the sum of counted grains. The zones are described down the section.

Zone 1 consists mostly of arboreal pollen dominated by *Pinus sylvestris*, with significant amounts of *Pinus sibirica* and *Larix* sp. (Fig. 13). The spectra of Zone 2 are dominated by *Pinus sibirica* and *Betula* sect. *Nanae* in the upper part, *Abies Sibirica*, *Larix* sp., *Picea obovata*, and *Salix* sp. in the middle, and *Picea obovata*, *Larix* sp., and *Ephedra* sp. pollen and Polypodicaceae spores in the lower part. Zone 3 is dominated by *Picea obovata*, *Larix* sp., and *Salix* sp. Spectra in Zone 4 are very poor and contain mostly wind-pollinated widely dispersed steppe and forest-steppe species, such as *Pinus sylvestris*, *Duschekia fruticosa*, Chenopodiaceae, and *Artemisia*. The spectra of Zone 5 are richer than in Zone 4 but contain much less arboreal pollen, predominantly *Duschekia fruticosa*, and herbal species of *Ephedra*, Chenopodiaceae, Caryophyllaceae, *Artemisia*, Cyperaceae, and Poaceae. Zone 6 is distinguished by notably higher percentages of *Picea obovata* and lower percentages of *Ephedra*. Zone 7 shows low percentages of arboreal pollen (dominated by *Betula*, *Duschekia*, and *Salix* species) and abundant herbs (Chenopodiaceae, Caryophyllaceae, *Artemisia*, Cyperaceae) and spores of *Polypodicaceae*. Zone 8 includes spectra with still lower (<30%) percentages of arboreal pollen dominated by *Pinus sylvestris* and *Pinus sibirica* but as much shrub alder and herbs, especially Chenopodiaceae, *Artemisia*, and Cyperaceae, and abundant spores of *Sphagnum* sp. Percentages of arboreal pollen in Zone 9 are higher (*Pinus sylvestris* and *Pinus sibirica*) but herbs are less abundant, especially Cyperaceae. Zone 10 shows spectra with high percentages of arboreal pollen (Fig. 13), mostly of *Pinus sylvestris*, *Pinus sibirica*, *Picea obovata*, and *Albies sibirica*.

Vegetation and climate reconstructions. The collected data were used for reconstructions of the vegetation and climate history of the expansive drainage basin of Lake Baikal. The deposition in the drill site was controlled by river input from the Selenga, the major lake tributary and the major pollen carrier, as well as from the Buguldeika, Bol'shaya Goloustnaya, and rivers originated on northern slopes of the Khamar-Daban Ridge. Interpretations of past vegetation and climate rested on a comparison of the pollen stratigraphy with modern spectra [33, 34] and with subrecent spectra from the Buguldeika, Bol'shaya Goloustnaya, and Khamar-Daban Ridge rivers, from Baikal bottom sediments [35], from Mongolia [36] and Transbaikalia [37].

The vegetation corresponding to Zone 11 cannot be reconstructed because of poorly representative spectra (Fig. 13), but we hypothesize landscapes of tundra with Chenopodiaceae, *Artemisia*, and Cyperaceae assemblages and open scarce forests with *Pinus sylvestris*, *Pinus sibirica*, and *Larix*. The zone formed during the Taz glacial.

At the onset of Zone 10, mid-mountain dark conifers of *Pinus sibirica* and *Albies sibirica* with fern cover and *Picea obovata* valley forests (Fig. 13) grew in a wet climate (mean annual precipitation at least 700 mm). Soil formation processes in improving climate conditions and permafrost degradation produced well drained ash-rich soils. High cyclonic activity may have been associated with changes in global atmospheric circulation in the northern hemisphere under the effect of the warm and wet North Atlantic circulation resumed in the interglacial. At the termination of Zone 10, *Pinus sylvestris*, *Pinus sibirica*, and *Larix* forests developed in a more continental cold and relatively dry climate.

During the deposition of Zone 9, forest vegetation became less abundant (Fig. 13). The forest-steppe assemblage may have included *Pinus sylvestris* and *Pinus sibirica* growing in wet subalpine conditions. Chenopodiaceae-*Artemisia* and *Poaceae* steppe assemblages became more abundant, and the appearance of *Ephedra* indicates desertification. Herbs, often *Caryophyllaceae*, which prefer dry turf-free conditions, likewise indicate a continental moderately cold dry climate with hot and dry summers and cold dry winters with little snow.

The cold and wet climate of Zone 8 caused swamping of near-delta plains, estuaries, and flood plains.
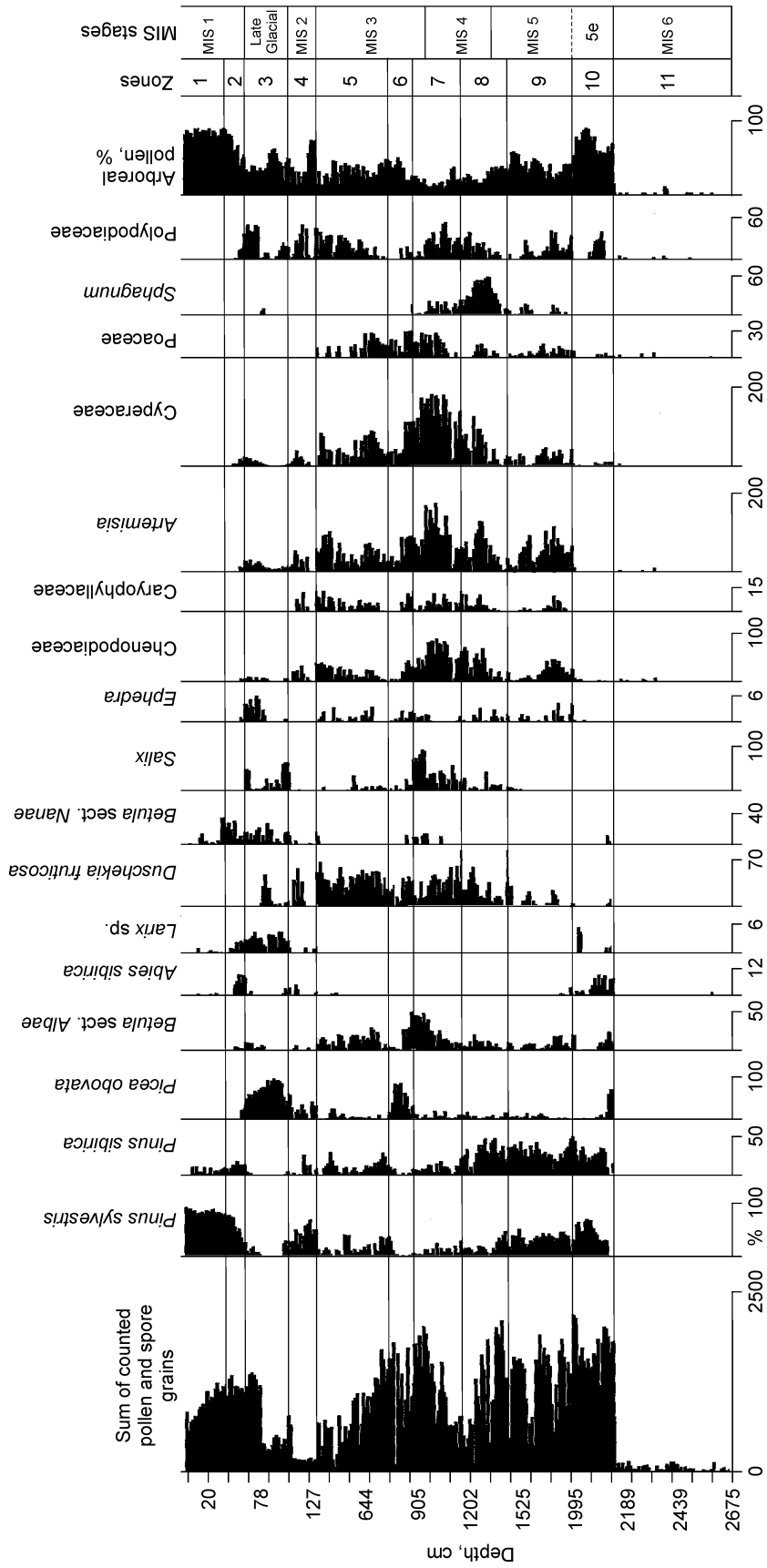
Fig. 13. Pollen percentage diagram for BDP-99 core at 0–25 m. Pollen zones on the right are correlated to marine oxygen isotope stratigraphy.

Abundant mesotrophic *Sphagnum* assemblages formed in superwet underdrain areas. Areas along river valleys and wet slopes were occupied by shrubs, mostly *Salix* and *Duschekia* species, steppe taxa grew in interfluves and on insolated mountain slopes, and the area of forests reduced considerably.

Lower percentages of arboreal pollen, including *Pinus sylvestris* and *Pinus sibirica* (Fig. 13), in Zone 7 indicate a larger spread of steppe, tundra, and forest-tundra vegetation. Shrub species of *Duschekia-Salix* tundra and *Betula* forest-tundra assemblages apparently occupied mid- and low-elevated mountains and river valleys. Cyperaceae, or occasionally *Sphagnum*-Cyperaceae eutrophic assemblages grew in swampy areas of estuarial plains and *Salix* developed in a stable well-drained hydrological regime. Vegetation in the Selenga basin was dominated by Chenopodiaceae and *Poaceae* steppe assemblages, possibly with scarce *Pinus sylvestris*, which grew in a strongly continental cold and relatively dry climate. Vegetation degraded in the conditions of permafrost expansion, low insolation, and poor snow covers.

The brief episode of enhanced forest growth, mostly *Picea obovata* valley forests (Zone 6, Fig. 13), may have been caused by slightly higher spring and summer temperatures and milder winters when the summer heat may have been sufficient for soil thawing, better drainage in swampy areas, larger spread of *Picea obovata* forests and reduced areas of *Sphagnum*-Cyperaceae marshes.

Vegetation in Zone 5 was dominated by forest-steppe and steppe assemblages, and *Pinus sibirica* forests occupied larger areas in mid-mountain taiga. Shrub assemblages grew on wet slopes, in river valleys and estuarine plains; *Betula* and *Pinus* species of forest-steppe, and *Poaceae-Artemisia* and Chenopodiaceae-*Caryophyllaceae* steppe assemblages developed in a dry moderately cold climate of Transbaikalian plains (Fig. 13).

The climate reconstruction for Zone 4 is less reliable because of few (2 to 125 spore and pollen grains in a standard slide) and poorly representative spectra (Fig. 13). Low pollen abundances may be accounted for by strongly reduced forest vegetation and dominant steppe and tundra assemblages. Then, *Pinus sylvestris* pollen must be exotic, transported from Mongolia or southern Transbaikalia.

High percentages of *Picea obovata* and *Larix* pollen, low percentages of *Pinus sylvestris* and *Pinus sibirica* and low pollen concentrations in Zone 3 (Fig. 13) indicate northern taiga and, possibly, forest-tundra landscapes in a cold moderately wet climate with extensive permafrost. *Abies sibirica*, *Pinus sylvestris*, and *Pinus sibirica* apparently occupied limited favorable subalpine areas, and shrub tundra species of *Alnus* and *Salix* occurred broadly. These reconstructions agree with those for many regions of Baikal, Siberia, and mid-latitude Eurasia during the time span from the onset of deglaciation about 15 kyr to the earliest Holocene (about 10 kyr) [38–45].

The onset of Zone 2 was marked by a brief highly arid episode indicated by high percentages of *Ephedra* typical of steppe and semi-desert flora, the highest in the BDP-99 core (Fig. 13). This excursion, possibly corresponding to the Younger Dryas, was followed by a wetter period of higher atmospheric precipitation, higher spring and winter temperatures, and a milder climate favorable for wet dark conifers with *Pinus sylvestris*, *Abies sibirica*, and Polypodiaceae.

During the accumulation of Zone 1 vegetation approached its modern composition dominated by forest taxa, mostly *Pinus sibirica*, *Pinus sylvestris*, and *Larix* (Fig. 13) growing in a relatively dry and moderately warm continental climate.

Composite section. A single composite record of the two cores was obtained based on drilling depth log and correlation of water and diatom contents [4] with reference to a conjugation point at 113 m, checked against diatom data.

The LDAZ 26-28 stratigraphy in BDP-96 corresponds to MIS 17. The succession of assemblages [26, 30] in these zones is critical for making up a composite section as they fall on the end of BDP-99-1 and the beginning of continuous coring in BDP-99-2. LDAZ 26 in BDP-99-1 ends at 113.27 m (Fig. 7); BDP-99-2 misses this diatom zone because of the core top loss (for details see "Drilling techniques"). However, double LDAZ 27-28 zone begins at 109.45 m in BDP-99-2. Since LDAZ 27 immediately follows Zone 26, it is reasonable to hypothesize that the second core is shifted 3.97 m above the first core. This correction is supported by the ~3.20 m depth difference of LDAZ 6 in BDP-99-1 and BDP-99-2: at 20.04 to 20.77 m in BDP-99-1 and at 16.96 to 17.39 m in BDP-99-2 (Fig. 7), and can be applied to the common BDP-99 depth scale.

The applicability of diatom stratigraphy as a check for the BDP-99-1 and BDP-99-2 composite section is confirmed by the diatom assemblage in section 12-1A (117.56–118.32 m) of BDP-99-2: The presence of *Cyclotella praeminuta* and *Stephanodiscus baicalensis* var. *concinnis* indicates that this interval belongs to 736–751 kyr LDAZ 29 in BDP-96-2 [26, 30]. Therefore, the distribution of diatom species in the composite BDP-99 section records the undisturbed stratigraphy of the Baikal sediments corresponding to MIS 17-18 (663–764 kyr). The specific diatom composition in section 16-1C (126.12–126.79 m) traces the succession of diatom zones in BDP-99 as far as LDAZ 31 corresponding to MIS 19 (780 kyr), at the Brunhes/Matuyama boundary (Fig. 7).

Thus, to obtain a composite section, data from BDP-99-2 starting from a depth of 109.45 m were added to

BDP-99-1 at the conjugation point of 112.14 m, plus 3.97 m of the depth shift between the diatom zones in both holes. The total length of the composite section is then 356.87 m. The top 1-1A section from BDP-99-2 was used to compensate the 15 cm core top loss in BDP-99-1.

DISCUSSION

Age model of BDP-99 section. Paleomagnetic data indicate a direct geomagnetic polarity in the upper BDP-99 section and a reversal at 234 m (Fig. 7). However, the earlier interpretation of this reversal as the 780 kyr Brunhes/Matuyama boundary [25] inferred from inclination records [46] disagrees with the diatom stratigraphy. The age of diatom layers at 170–220 m core depth is 0.9–1.12 myr, far beyond the Brunhes Chron.

A preliminary age model of BDP-99 was constructed on the basis of the BDP-99 lithology, biostratigraphic correlation of BDP-99 with BDP-93 and BDP-96, and inclination profiles. The upper units in BDP-99 and BDP-93 have similar thicknesses, though sedimentation rates within some time intervals were different. The last interglacial (Kazantsevo time, LDAZ 6 [26, 30]) begins at ~18 m in BDP-93 [47] and at 20–21 m in BDP-99-1. The interglacial corresponding to MIS 11, recorded by LDAZ 17-18 in the Baikal cores [26, 30], is at 68–71 m in BDP-93 [48] and at 58–62 m in BDP-99-1. The basal age of the 100 m BDP-93 core is about 660 kyr [6, 18, 49], and in BDP-99-1 this age corresponds to the interval between 112 and 114 m (LDAZ 26) (Fig. 7).

Therefore, coeval layers in the two boreholes were deposited at different rates, some intervals formed faster at the Buguldeika site and others on the Posol'sk Bank. However, the mean sedimentation rates differ for no more than 10%: The deposition of the 100 m thick Buguldeika section lasted 660 kyr at a mean rate of 15.15 cm/kyr and the 126 m thick Posol'sk Bank section was deposited for 789 kyr (Fig. 7) at 16.16 cm/kyr.

Unlike the BDP-96 and BDP-98 records, BDP-99 does not show the expected polarity reversal from the direct Brunhes to the reverse Matuyama epoch below LDAZ 29-31. Instead, the reversal within LDAZ 31 (Brunhes/Matuyama boundary) looks rather as a magnetic excursion underlain by the following direct polarity interval. Taking into account the reliable correlation of the Upper and Lower Pleistocene markers in BDP-99 and BDP-96, the disturbed succession in the BDP-99 inclination profile can be attributed to a deposition gap between the upper and the lower units of the Posol'sk Bank section.

Correlation of the top 0–3 m in BDP-99 and BDP-93 (Fig. 8) shows that the postglacial sections have almost the same thicknesses and were deposited at similar mean rates (about 15 cm/kyr in BDP-99 and about 17.6 cm/kyr in BDP-93) [47].

The short reverse polarity interval corresponding to LDAZ 31 may be the upper part of the Matuyama Chron [26]. On the other hand, the BDP-99 core misses a considerable portion of sediments corresponding to the Matuyama epoch, as the new direct polarity interval spans the section between 134 m and 234 m. Therefore, the core depth of 134 m in BDP-99 corresponds to an unconformity, and the intermediate unit is most likely a part of the 0.99–1.5 myr Jaramillo direct polarity chron [50]. This interpretation is supported by the diatom stratigraphy indicating the presence of 0.9–1.12 myr Baikal species typical of the Jaramillo Subchron (Fig. 7).

The discovery of a hiatus in the BDP-99 section on the uplifted block of the Posol'sk Bank, a loss of an ~200 kyr interval according to the preliminary age model, is the first and the best prominent in the history of the Baikal project. The hiatus occurs at the boundary between the upper and intermediate units and is marked by an abrupt change in lithology, color, water content, and diatom abundances of the sediments. The 120 m section below the hiatus should have been deposited for the short Jaramillo Subchron at extremely high mean sedimentation rates (~1.7 m/kyr). The basal age of the BDP-99 section is as yet difficult to constrain. It may be estimated at about 1.2–1.3 myr taking into account the mean sedimentation rate during Jaramillo time and the presence of a greater number of turbidite layers in the lower section (unit 1, Figs. 6, 7).

Paleoclimate signals in the BDP-99 section. Piston coring and later studies of deep Baikal cores show a rhythmic sedimentary section made up by alternation of diatomaceous mud with diatom-barren clay [1–4, 51]. The rhythmic structure of the Academician Ridge cores was traced to depths of 600 m [4], and diatom-rich layers were attributed to warm interglacial times and clays to glacials [1–6]. A rhythmic pattern in the BDP-99 core is well pronounced in the upper 87 m.

The correlation of BDP-99 with the Academician Ridge section, the composite section of the two Posol'sk Bank holes, and the age model are based on local diatom zones marked by indicator species [26]. The main diatom species are encountered throughout the lake (Academician Ridge, Buguldeika Saddle, Posol'sk Bank) and are tied to age, namely in a model age scale for the Brunhes Chron constructed for BDP-96 [52]. *Stephanodiscus grandis*, *S. formosus*, *S. carconeiformis*, *Synedra ulna* var. *danica*, and *A. islandica* of LDAZ 6 are encountered in the Academician Ridge, Buguldeika Saddle, and Posol'sk Bank cores and are attributed to the warm stage of MIS 5e (120–130 kyr), as well as species of LDAZ 12-13, 14, 17-18, etc. (see the section "Preliminary diatom

stratigraphy"). Diatoms became virtually extinct during glacials [26, 27, 30, 31] and were absent from the pelagic regions, but some preserved occasionally in shallow bays and gulfs better warmed-up in summer months. On the other hand, the formation of new species simultaneously in distant parts of the lake in interglacial times indicates that similar favorable environments for speciation and expansion of diatoms existed in different lake regions despite the great size of Baikal, which is possible in a single pelagic ecosystem. The existence of a single ecosystem with the same response to climate change makes the diatom stratigraphy applicable to correlation of cores from different parts of the lake. However, some species (e.g., *Aulacoseira italica*) found in the LDAZ 6 assemblage are restricted to BDP-99, possibly, because of the influence of large river input (mostly from the Selenga) on the development of other non-endemic diatom species. This fact should be taken into account in paleoclimatic reconstructions for different geomorphic settings of Lake Baikal.

It was noted [1–4] that diatom-rich layers have higher water contents than clay, and this was used as a simplified climate proxy in the BDP-96 core [23]. Figure 11 shows the BDP-99 diatom abundance and water content curves compared to the BDP-96-2 biogenic silica curve for the 0 to 800 kyr time span, and an ODP-677 $\delta^{18}O$ curve [50], which allows correlation of BDP-99 with the marine oxygen isotope stratigraphy and demonstrates the reliability of the BDP-99 age model. Glacials and interglacials distinguished for Siberia [39, 53, 54, 58] (Fig. 10) correlate well with the stages and substages of the marine oxygen isotope curve [52] (Fig. 11, on the right). The resulting paleoclimate record from the Posol'sk Bank displays many climate events distinguished earlier in the cores from the Academician Ridge [3, 4, 6, 10].

The BDP-99 diatom and water content curves show thin clay layers with low diatom and water contents inside warm MIS 5 and 7 at 18–19.5 and 35.6–39.4 m (Fig. 11) deposited during glacial excursions of substages 5d (105–117 kyr) and 7d (220–232 kyr) [10, 18, 55]. These brief but deep cooling events caused by lower insolation [56] are weakly pronounced in marine records but clearly expressed in many continental archives [57]. The insolation-controlled excursions in Siberia were accompanied by mountain glaciation [10, 18, 53, 58, 59] and are also found in the Posol'sk Bank record. Note that deposition of a thicker layer of glacial clay during 7d (220–232 kyr) than during 5d indicates a longer and deeper glaciation, in BDP-99 as well as in the Academician Ridge cores, and agrees with a greater insolation decrease in 7d [56]. This agreement is evidence for high sensitivity and reliability of the Posol'sk Bank records. Moreover, the presence of glacial layers in different sections throughout Baikal indicates that glaciation was not restricted to the Northern subbasin surrounded by glaciated mountains. Mountain glaciation in the Khamar-Daban Ridge, northwestern Mongolia, and eastern Tuva, i.e., in the regions drained by the Selenga, the largest Baikal tributary, may have controlled the supply of glacial clays into the Central and South subbasins of the lake and to the Posol'sk Bank.

Diatom abundances is a reliable climate proxy for the 0–800 kyr time span (Fig. 11), but diatoms in the lower section are much less abundant and poorly preserved, with traces of dissolution in many intervals. In this respect the preservation of diatoms and the causes of their absence from some core depths are worth of special attention.

Diatom abundance variations in the Academician Ridge cores correlate well with climate change and the recorded signals may be produced by climate-driven diatom production. Most diatoms become dissolved in the water column and only few settle down but remain buried as climate signature in the bottom sediments [60]. Low sedimentation rates (about 4 cm/kyr) on the Academician Ridge provide important conditions for the preservation of diatoms in the sedimentary section.

High contents of the terrigenous component and dilution with terrigenous material in the lower Posol'sk Bank section might be responsible for low diatom contents (Fig. 7) but cannot be the only cause. At a high terrigenous flux and an approximately constant diatom production in the water column, the abundances of diatoms per gram sediment decrease but the diatom layers become thicker. However, the diatom abundances in the lower part of the BDP-99 core decrease and the diatom layers become thinner (Figs. 7, 11), which indicates terrigenous dilution along with lower diatom deposition.

A part of decrease in diatom contents may be due to dissolution of diatoms in sediments, observed in the shallow section [61], and the lower the diatom concentration the stronger the dissolution. Terrigenous dilution may thus produce lower concentrations and more intense dissolution of diatoms. This double effect of dilution and dissolution is apparently responsible for the low diatom abundances in the Posol'sk Bank and Buguldeika cores.

At the same time, dissolution of diatoms in the sediment was almost never observed in the Academician Ridge cores, i.e., the low diatom contents and their partial dissolution in the lower sections of the Buguldeika and Posol'sk Bank cores may be a local phenomenon, most likely associated with a high terrigenous flux near the Selenga delta. This makes diatom abundances a less reliable climate proxy in the lower section, but palynological and geochemical proxies remain workable being independent of terrigenous dilution.

Up to now palynological records are available only for the uppermost BDP-99 section, but even this limited

amount of data has been an important clue to past climates. Spore-pollen compositions correlated with diatom and water contents (Figs. 11, 13) show that the sampled 25 m of the core span the interval of MIS 1-6, or 0 to 150 kyr. Therefore, pollen Zone 1 and the termination of Zone 2 correspond to the Holocene and MIS 1, and the onset of Zone 2 — Zone 3 to the Last Glacial. The spectra of Zone 4 record the maximum of the Sartan glacial (MIS 2). Then, Zones 5–6 and the second half of Zone 7 are correlated with the Karga interstadial (MIS 3), the first half of Zone 7 and the termination of Zone 8 with the Zyryanka stage or MIS 4, and the onset of Zone 8 and Zones 9–10 with the Kazantsevo interglacial (MIS 5). The 5e signal, apparently corresponding to pollen zone 10, is the most prominent within MIS 5. The reconstruction for that time indicates a wet, moderately warm and moderately continental climate with mild snowy winters, cool summers, and limited and shallow permafrost. These conditions were favorable for dark conifers dominated by fir, pine, and spruce species. Spectra of a similar composition typical of the wet Holocene optimum from 8.5 to 4.5 kyr were observed in earlier studies of Baikal bottom sediments and lacustrine and bog deposits from the Baikal catchment [62–65, etc.].

Pollen spectra in the BDP-99 cores contain diverse pollen species from dramatically different environments: Wet forest, deltaic, flood-plain, tundra and forest tundra taxa coexist with plants from dry forest-steppe, steppe, and even semidesert regions. This intricate composition is produced by plant assemblages from the mountainous surroundings of Lake Baikal and from the large catchment of the Selenga which drained the territory dominated by forest-steppe, steppe, and semidesert landscapes in the Pleistocene. Dark conifers grew profusely in the moderately wet and cool climate of the 5e substage, in the Early and Middle Holocene mid-mountain taiga around Baikal [35], and in mountains of Mongolia [66].

Correlation of the BDP-99 cores with seismic sections. Deep cores from Lake Baikal provide a unique opportunity for the interpretation of the available seismic data and their extrapolation onto large areas of the lake's bottom. Unfortunately, none of the earlier seismic profiles crosses the very drill site of BDP-99, but the nearest are seismic lines 91-19 and 92-67 (Fig. 1) collected during joint Russian-American cruises on the R/V *Vereshchagin* in 1991 and 1992 [16, 17].

Acoustic velocities is a key point in the correlation of seismic and core data. Calculations are most often based on sound velocity in water, about 1500 m/s. Direct acoustic measurements in BDP-98 (Academician Ridge) show that acoustic velocities in bottom sediments at subbottom depths of 0–250 m vary from 1625 to 1650 m/s [67].

The estimated acoustic velocities in the BDP-99 section in 201 m of water, at a sediment thickness of 250 m, vary from 1535 to 1570 m/s (mean velocities including a 200 m water column). The depths of seismic boundaries were estimated assuming a velocity of 1550 m/s [Pevzner, pers. commun.], which allows precise referencing to the core lithology and stratigraphy.

Single-channel seismic profiling. Figure 3 shows the position of the BDP-99 hole relative to line 92-67 of single-channel water-gun continuous seismic profiling. The borehole penetrates several seismoacoustic units corresponding to different lithologies.

Unit I (Fig. 3) marked by prominent reflections is a thickly layered section of the upper 29 m of the core composed of diatomaceous mud (20–47% diatoms) alternating with glacial-lacustrine clay. Strong reflections may be produced by variations in density and water contents (Figs. 9–11) correlated with diatom abundances: High water contents in less dense diatom-rich layers and low water contents in dense clay.

Diatom abundances and water contents decrease and become less variable down the section (Figs. 7, 9–11) and the density jumps and the reflections are less prominent (Fig. 3). Therefore, Unit II has weaker reflectors and Unit III is almost transparent (Fig. 3). Unit II corresponds to depths between 29 and 87 m in which diatom-rich (25–40%) mud alternates with dense clay (Figs. 7, 9–11).

Unit III (87–180 m) is more uniform and is composed of dense clay intervened with thin silt layers (5–15% diatoms) (Fig. 7). Weak variations in water contents produce the weakest reflections.

Unit IV (180–232 m) shows discontinuous and poorly traceable but stronger reflectors (Fig. 3, *B*), possibly due to sand enrichment in the lower section (Fig. 6). The resolution is relatively low, because water content and density variations are weak, and because of technological limitations of the acquisition system. Diatom percentages in Unit IV are low (~5–15%) (Fig. 7). Acoustic signal disappears below 232 m (Fig. 3).

The acoustic record generally agrees with the lithology and the physical properties of sediments. The boundaries of the seismic units almost perfectly coincide with the diatom and water content boundaries, which allows precise correlation and age referencing.

At the same time, the seismic section does not image the hiatus recorded in the core at 134 m (Fig. 7). In the seismic section this depth falls into the middle of Unit III (Fig. 3) with obscure layering. The section shows no traces of a gap immediately in the drill site but an unconformity is recorded upslope, where the acoustic signal is clearer. The unconformity may continue downslope but remain undetectable in the seismic record.

Age of acoustic units. The age of the distinguished seismoacoustic units and their correlation with climate

events can be inferred from the depths of their boundaries and diatom stratigraphy (Figs. 7, 11). The lower boundary of Unit I at a subbottom depth of 29 m where a water content change is marked by a reflector (Fig. 11) corresponds to the middle of MIS 6 (Taz glacial). Therefore, the basal age of the unit is 150 kyr, i.e., it was deposited during the Late Pleistocene-Holocene (0–150 kyr).

The boundary between Units II and III at ~87 m corresponds to the MIS 15a/15b boundary dated at 583 kyr (Fig. 11). It is difficult to correlate this boundary to the Siberian stratigraphic scale but according to the age it may correspond to the mid-Til'tim interglacial [52, 53, 57]. Thus, Unit II spans the interval from 150 to 583 kyr (Middle Pleistocene).

The boundary between Units III and IV at 180 m coincides with the ~1.07 myr lower boundary of the diatom zone *Stephanodiscus williamsii*, *S. yukonensis* var. *antiquus*, *Synedra ulna* var. *danica* (Fig. 7), and the lower boundary of Unit IV at 234 m corresponds to the lower boundary of the *Cyclotella ocellata*, *Aulacoseira subarctica* zone with the diatom stratigraphy age of 1.12 myr (Fig. 7). Therefore, Unit III was deposited from 0.58 to 1.07 myr (Early-Middle Pleistocene) and Unit IV between 1.07 and 1.12 myr (Early Pleistocene).

High-resolution seismic profiling. Figures 4 and 14 show the position of the BDP-99 drill site relative to the water-gun high-resolution profile 91-19. The section contains several reflectors* whose depths can be inferred from acoustic velocity. The age of acoustic boundaries is estimated on the basis of their depths and correlation with the diatom stratigraphy of BDP-96-2 (Fig. 11).

The depth of the first acoustic boundary on the high-resolution record (CSP profile 91-19) is at ~21 m and corresponds to the ~130 kyr boundary between MIS 6 (Taz glacial) and 5e (Kazantsevo interglacial) (Figs. 11, 14). The age of the lowermost acoustic unit in 91-19 is about 360 kyr and corresponds to the end of MIS 11 (Tobol interglacial) — beginning of cold MIS 10. The ages and depths of intermediate acoustic boundaries (Fig. 14) are perfectly correlated with the water content and density boundaries on transition from clay to diatomaceous mud.

The relatively uniform structure of the uppermost Posol'sk Bank section allows us to extrapolate the age estimates up and down the slope and to time the layers that pinch out on the steep southwestern slope of the bank (Fig. 4, *B*). The top acoustic unit in 91-19 (Unit I, 0–130 kyr) thins down upslope and is truncated by erosion. In the drill site, this unit encompasses sediments deposited between MIS 1 (Holocene) and late MIS 6 (Taz glacial), including the Sartan glacial (MIS 2), the Karga interstadial (MIS 3), the Zyryanka glacial (MIS 4), and the Kazantsevo interglacial (MIS 5). Figure 4 shows that a number of layers in the upper unit die out gradually, and the deposits of MIS 6 located below the first seismic boundary (Fig. 4) become exposed on the top of the Posol'sk Bank.

Therefore, the exposed clays under 35 m of water were deposited during the Taz glacial of the Siberian stratigraphic scale (Fig. 11) [39, 53, 54, 58] and have an age of 130–180 kyr rather than belong to the 11–24 kyr Sartan glacial (MIS 1) as we thought before. Several unconformities on the top of the Posol'sk Bank where the upper layers truncate the sediments below (Figs. 3, 4) may correspond to past episodes of low stand which can be timed from the ages of the seismic units.

Deposition environments and tectonic activity in the Posol'sk Bank region. The cored sedimentary section of the Posol'sk Bank documents the tectonic history of the region, unlike the previous cores from the Buguldeika Saddle, the Academician Ridge, and the South Baikal basin, except for the 600 m BDP-98 core spanning 8 myr [4, 68]. The BDP-98 record displays gradual changes in the deposition environments associated with changes in the tectonic setting and surface topography. The BDP-99 core containing an unconformity followed by a sharp decrease in sedimentation rate offers a unique opportunity to time the causative tectonic event.

The whole BDP-99 section was deposited in submarine conditions indicated by the reduced colors of sediments (black-olive to gray) and the absence of subaerial facies. However, the deposition environment on the Posol'sk Bank underwent considerable changes. The upper 134 m section was deposited in an environment similar to the present-day one which persisted through the past 820 kyr, and the deposition of the intermediate and lower sections (134–325 m) occurred at a terrigenous input higher than it is now. High sedimentation rates and the lithological uniformity of the lower and intermediate units indicate a relatively stable sediment transport from a nearby source between 0.82 and 1.3 myr. The sedimentary material deposited at an extremely high rate of 1.7 m/kyr was most likely supplied as suspended particles by the Selenga, the major Baikal tributary. The morphology of the Selenga region was possibly different from the present-day setting, and the BDP-99 site was located on the path of direct river input. An environment similar to distal deltaic conditions is indicated by the presence of sand and turbidite layers in the lower BDP-99 section. Since 0.82 myr the deposition on the slope of the Posol'sk Bank became

---

*   The depths of the reflectors in 92-67 and 91-19 not always coincide as the profiles were collected using different acquisition systems and are at some distance apart.
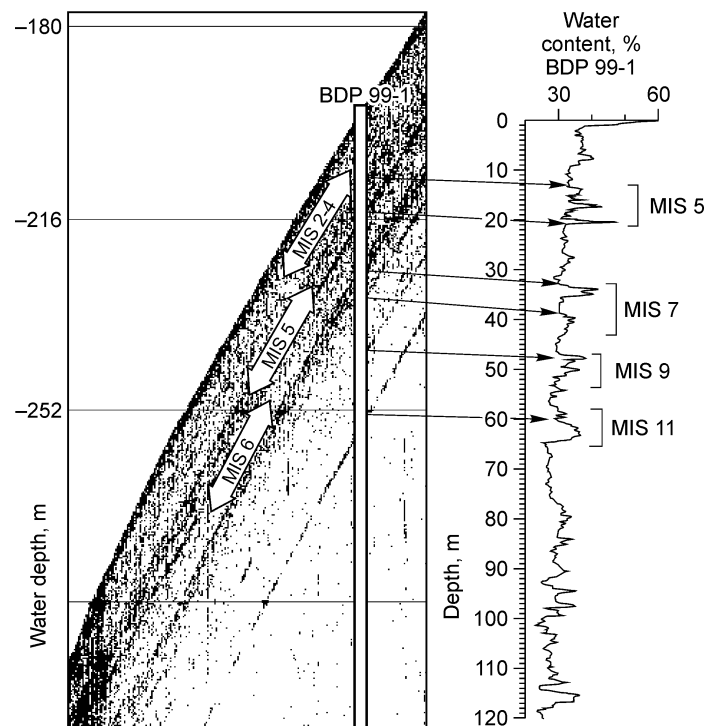
Fig. 14. Possible correlation of high-resolution continuous seismic reflection profile 91-19 [16, 17] with water content in BDP-99 core. Position of seismic profile is shown in Fig. 1. MIS 5–MIS 11 show position of seismic units corresponding to marine oxygen isotope stages.

controlled more by settling of terrigenous particles brought by lake currents than by direct river input, and the sedimentation rate became ten times as low (~16 cm/kyr).

The erosional unconformity at 134 m that separates the upper hemipelagic and the intermediate deltaic units may mark a tectonic restructuring of crustal blocks in the Selenga region. It appears reasonable to correlate this tectonic event with the erosional boundary D2B distinguished by Scholz and Hutchinson [13] which we erroneously called D3B in [6]. The earlier 1.07–1.31 myr ages of this boundary (1.12 myr for the whole Selenga region [13]) were inferred by extrapolation of sedimentation rates from the Buguldeika Saddle (BDP-93) [6]. These estimates were updated using BDP-99 data which constrain the tectonic event between 820 kyr and 1 myr. Therefore, the age of the unconformity in BDP-99 approaches the average age of D2B inferred from multichannel seismic profiling data [13] and corresponds to the time of uplift of the Primorsky Ridge [69, 70].

The surface topography and the deposition environment changes may have been associated with the rapid uplift of the eastern slope of the Posol'sk Bank half-horst along the Posol'sk fault and the subsidence of the western side of the graben in the northern termination of the South Baikal subbasin. Prior to the uplift, the slope of the Posol'sk Bank was part of the submerged slope of the Selenga delta, the area of fluvial deposition. As a result of the uplift and the subsidence, the South Baikal subbasin advanced toward the delta and separated the bank from the latter.

The lower and intermediate units of the BDP-99 section (134–350 m) may have deposited on the slope of the paleo-Selenga river by direct sediment input and record a deltaic environment, whereas the upper 134 m of the section formed in hemipelagic conditions by the settling of suspended terrigenous particles from the water and diatom production, i.e., in a limnic environment, though under a considerable influence of the river input. This difference in deposition environments accounts for the difference in lithology and in the contents and preservation of diatoms. Deposition on the submerged delta slope was dominated by terrigenous input and diatom sedimentation was of secondary importance. Transport of diatoms may have been accompanied by their motion downslope, disintegration, and subsequent dissolution, which explains the poor preservation of diatom frustules and the abundance of their fragments in the lower section.

The present-day fault scarp on the southeastern slope of the Posol'sk Bank is over 900 m high. The rate of the uplift of the eastern bank side inferred from the duration of the deposition gap (about 200 kyr) is at least 4.5 mm/yr, slower than the uplift of rift ridges around Lake Baikal (8.9–27.4 mm/yr) [71]. This event was concurrent with the Primorsky tectonic episode of the neo-Baikalian rifting stage marked by the abrupt acceleration of the Primorsky Ridge uplift, the restructuring of the drainage network, and the cessation of Baikal discharge through the paleo-Manzurka [69, 70].

The glacial-lacustrine clay in BDP-99 is lithologically similar to those from the Academician Ridge. Accumulation of this clay in southern Baikal, far from the direct effect of glaciers, indicates that the influence of glaciation involved whole Baikal rather than being restricted to its northern subbasin surrounded by glaciers in the Pleistocene [69]. Glacial clay may have been supplied into South Baikal as ice-rafted material, from the Khamar-Daban Ridge glaciers, or transported by the Selenga that entrained melt water from the eastern Khamar-Daban slopes and from Mongolian mountains. Traces of ice rafting in the glacial-lacustrine clay from the Posol'sk Bank (sand lenses, gravel and pebble particles) indicate the existence of numerous icebergs during glacials. The icebergs may have originated from North Baikal glaciers [70, 72, 73] or from glaciers of the Southern subbasin.

CONCLUSIONS

The BDP-99 drilling experiment on the slope of the Posol'sk Bank yielded a 350 m core spanning an interval about 1.2–1.3 myr. The obtained diatom stratigraphy and paleomagnetic data show a ~200 kyr deposition gap at 134 m subbottom depth, though the Brunhes Chron of direct polarity (0–780 kyr) is complete. The 120 m of sediments below the gap were deposited at a very high rate of 1.7 m/kyr in the average.

The deposition gap revealed on the uplifted block of the Posol'sk Bank is the first and the best prominent unconformity in the Baikal cores retrieved in the BDP experiments. The presence of the gap indicates that the causative tectonic event in the Selenga region occurred between 0.8 and 1.0 myr, which corresponds to the time of uplift of the Primorsky Ridge estimated from land data [69, 70]. The uplift occurred at a rate at least 4.5 mm/yr.

The correlation of the BDP-99 core with the diatom stratigraphy of BDP-96-2 (Academician Ridge) located over 200 km far away in a region with different water depths and different summer temperatures of surface waters attests to simultaneous development of planktonic diatoms throughout the lake on the geological time scale. Therefore, pelagic Baikal has had a single ecosystem with a synchronous and uniform response to climate events, which makes the diatom stratigraphy applicable to correlation of cores from different parts of the lake, as well as to dating within the Brunhes Chron and correlation with the marine oxygen isotope record.

High sedimentation rates in the BDP-99 core and high-resolution palynological sampling make a basis for detailed reconstructions of climate and environment changes in the Baikal basin and its surroundings.

Correlation of the BDP-99 section with seismic reflection profiles places constraints on the age of the seismoacoustic units and the reflectors and allows extrapolation of these age estimates on the whole Posol'sk Bank.

Further studies of the BDP-99 core are planned to investigate the response of the Baikal ecosystem to climate change in the region of intense biogenic input from the land, the Selenga runoff, and the atmospheric precipitation in the Selenga drainage basin.

REFERENCES

1. BDP-93 Working Group, Preliminary results of first drilling on Lake Baikal, Buguldeika isthmus, *Geologiya i Geofizika (Russian Geology and Geophysics)*, **36**, 2, 3–32(1–30), 1995

2. BDP-93 Baikal Drilling Project Members. Preliminary results of the first drilling on the Lake Baikal, Buguldeika site, south-eastern Siberia, *Quatern. Inter.*, **37**, 3–17, 1997.

3. The Baikal Drilling Project Group, A continuous record of climate changes for the last five million years from the bottom sediments of Lake Baikal, *Geologiya i Geofizika (Russian Geology and Geophysics)*, **39**, 2, 139–156(135–152), 1998.

4. Baikal Drilling Project Group, Late Cenozoic paleoclimate record in bottom sediments of Lake Baikal (600 m of deep drilling data), *Geologiya i Geofizika (Russian Geology and Geophysics)*, **41**, 1, 3–32(1–29), 2000.

5. Kuz'min, M.I., G.V. Kalmychkov, A.D. Duchkov, V.F. Geletiy, A.Y Gol'mshtok, and E.B. Karabanov, Methane hydrates in Baikal sediments, *Geologiya Rudnykh Mestorozhdeniy*, **42**, 1, 25–37, 2000.

6. Kuz'min, M.I., E.B. Karabanov, A.A. Prokopenko, V.F. Geletiy, V.S. Antipin, D.F. Williams, and A.N. Gvozdkov, Sedimentation process and the new age constraints on rifting stages in Lake Baikal: the results of the deep-water drilling, *Int. J. Earth Sci.*, **89**, 183–192, 2000.

7. Karabanov, E.B., A.A. Prokopenko, D.F. Williams, and G.K. Khursevich, A new record of Holocene climate change from bottom sediments of lake Baikal, *Palaeogeography, Palaeoclimatology, Palaeoecology*, **156**, 1211–1224, 2000.

8. Prokopenko, A.A., M.I. Kuz'min, E.B. Karabanov, and D.F. Williams, The response of the Lake Baikal sedimentary record to the Heinrich event in the North Atlantic for the past 80 kyr, *Dokl. RAN*, **379**, 3, 391–397, 1996.

9. Williams, D.F., J.A. Peck, E.B. Karabanov, A.A. Prokopenko, V.A. Kravchinsky, J. King, and M.I. Kuz'min, Lake Baikal record of continental climate response to orbital insolation during the past 5 million years, *Science*, **278**, 1114–1117, 1997.

10. Karabanov, E.B., A.A. Prokopenko, D.F. Williams, and S.M. Colman. The link between insolation, North Atlantic circulation and intense glaciations in Siberia during interglacial periods of Late Pleistocene, *Quatern. Res.*, **50**, 46–55, 1998.

11. Prokopenko, A.A., E.B. Karabanov, D.F. Williams, and G.K. Khursevich, Continental response to Heinrich events and Bond cycles in the sedimentary record of Lake Baikal, Siberia, *Global and Planetary Changes*, **28**, 217–226, 2002.

12. Zonenshain, L.P., A.Ya. Gol'mstock, and D.R. Hutchinson, The structure of the Baikal rift, *Geotektonika*, **5**, 63–77, 1992.

13. Scholz, C.A., and D.R. Hutchinson, Stratigraphic and structural evolution of the Selenga Delta accommodation zone, Lake Baikal rift, Siberia, *Int. J. Earth Sci.*, **89**, 212–228, 2000.

14. Bogdanov, Yu.A., and L.P. Zonenshain, Outcrops of Miocene sediments on the bottom of Lake Baikal and timing of faulting (observations from "Pisces" manned submersibles), *Dokl. AN*, **320**, 931–933, 1991.

15. Scholz, C.A., K.D. Klitgord, U.S. Ten Brink, L.P. Zonenshain, A.Ya. Golmshtok, and T.C. Moore, Results of 1992 seismic reflection experiment in Lake Baikal, *EOS*, (Transactions, American Geophysical Union), **74**, 465–470, 1993.

16. Colman, S.M., D.S. Foster, and J. Hatton, High-resolution seismic-reflection surveys of Lake Baikal, Siberia, 1990–1992, *USGS Open-file report 96-274*, 1–21, 1996.

17. Colman, S.M., D.S. Foster, and J. Hatton. High-resolution seismic-reflection surveys of Lake Baikal, Siberia, 1990–1992, *US Geological Survey Open-File Report 96-274*, 1996, http://geo-nsdi.er.usgs.gov/metadata/open-file/96-274/metadata.faq.html

18. Karabanov, E.B., *Geology of the bottom sediments of Lake Baikal and reconstruction of Cenozoic climate change in Central Asia* [in Russian], Abstract, Doctor Thesis, 72 pp., Institute of Lithosphere RAS, Moscow, 1999.

19. Potemkina, T.G., and V.A. Fialkov, Balance of river sediment load in the Selenga Delta and their distribution in Lake Baikal, *Vodnye Resursy*, **20**, 6, 689–692, 1993.

20. Potemkina, T.G., and V.A. Fialkov, Distribution of river sediment load in streams of the Selenga Delta and their transport to Lake Baikal, *Geografiya i Prirodnye Resursy*, 2, 70–74, 1998.

21. Terry, R.D., and G.V. Chilingar, Summary of "Concerning some additional aids in studying sedimentary formations" by M.S. Shvetsov, *J. Sedim. Petrol.*, **25**, 229–234, 1995.

22. Scholle, P.A. A color illustrated guide to constituents, textures, cements and porosities of sandstones and associated rocks, *AAPG Memoir*, **28**, ii–vii, 1979.

23. Kuz'min, M.I., M.A. Grachev, and D.F. Williams, A continuous paleoclimate record of the past 4.5 Ma from Lake Baikal, *Geologiya i Geofizika (Russian Geology and Geophysics)*, **38**, 5, 1021–1023(1062–1064), 1997.

24. Grachev, M.A., S.S. Vorobyova, Y.V. Likhoshway, E.L. Goldberg, G.A. Ziborova, O.V. Levina, and O.M. Khlystov, A high-resolution diatom record of the paleoclimates of East Siberia of the last 2.5 Myr from Lake Baikal, *Quatern. Sci. Rev.*, **17**, 1101–1106, 1998.

25. Cande, S.C., and D.V. Kent, Revised calibration of the geomagnetic polarity time scale for the Late Cretaceous and Cenozoic, *J. Geophys. Res.*, **100**, 6093–6095, 1995.

26. Khursevich, G. K., E.B. Karabanov, A.A. Prokopenko, D.F. Williams, M.I. Kuz'min, S.A. Fedenya, A.N. Gvozdkov, and E.V. Kerber, Detailed diatom biostratigraphy of Baikal sediments during the Brunhes Chron and climatic factors of species formation, *Geologiya i Geofizika (Russian Geology and Geophysics)*, **42**, 1, 108–129(97–116), 2000.

27. Khursevich, G.K., E.B. Karabanov, A.A. Prokopenko, D.F. Williams, M.I. Kuz'min, and S.A. Fedenya, Biostratigraphic significance of new fossil species of the diatom genera *Stephanodiscus* and *Cyclotella* from Upper Cenozoic deposits of Lake Baikal, Siberia, *Micropaleontology*, **47**, 47–71, 2000.

28. Prokopenko, A.A., D.F. Williams, and E.B. Karabanov, Response of Lake Baikal ecosystem to climate forcing and p_{CO_2} change over last glacial/interglacial transition, *Earth Planet. Sci. Lett.*, **172**, 239–253, 1999.

29. Colman, S.M., G.A. Jones, M. Rubin, J.W. King, J.A. Peck, and W.H. Orem, AMS radiocarbon analyses from Lake Baikal, Siberia: challenges of dating sediments from a large, oligotrophic lake, *Quatern. Sci. Rev. (Quaternary Geochronology)*, **15**, 669–684, 1996.

30. Khursevich, G.K., E. B. Karabanov, A.A. Prokopenko, D.F. Williams, M.I. Kuz'min, S.A. Fedenya, and A.N. Gvozdkov, Insolation regime in Siberia as a major factor controlling diatom production in Lake Baikal during the past 800 000 years, *Quatern. Inter.*, **80–81**, 47–58, 2001.

31. Khursevich, G.K., E. B. Karabanov, D.F. Williams, M.I. Kuz'min, S.A.Fedenya, A.A. Prokopenko, Evolution of freshwater centric diatoms during the Late Cenozoic within Baikal Rift Zone, *Proceedings of BICER, BDP and DIWPA Joint International Symposium on Lake Baikal, 1998 year,* Yokohama, Japan, 146–154, 2000.

32. Faegri, K., and J. Iversen, *Textbook of Pollen Analysis, fourth edition*, (revised by K. Faegri, P.E. Kaland, and K. Krzywinski), Wiley&Sons, Chichester, 431 p., 1989.

33. Galasiy, G.I. (ed.), *Atlas of Lake Baikal* [in Russian], 160 pp., FSGKR, Moscow, 1993.

34. Vorob'ev, V.V., and A.V. Martynov (eds.), *Nature management and environment conservation in the drainage basin of Lake Baikal* [in Russian], 221 pp., Nauka, Novosibirsk, 1990.

35. Bezrukova, E.V., *Last Glacial and Holocene paleogeography of the Baikal region* [in Russian], 128 pp., Nauka, Novosibirsk, 1999.

36. Savina, L.N., and T.A. Burenina, Preservation of *Larix* pollen in forest soils and the record of the composition of deciduous forests of Mongolia in recent spectra, in *Paleobotanic studies in forests of North Asia* [in Russian], ed. L.N. Savina, 62–83, Nauka, Novosibirsk, 1981.

37. Stefanovich, E.N., Comparative analysis of spore-pollen spectra from modern slope deposits in the taiga zone, in *Palynology in geomorphological studies* [in Russian], Moscow University Press, Moscow, 1971.

38. Gerasimov, I.P., and A.A. Velichko (eds), *Paleogeography of Europe for the past 100 kyr. Atlas* [in Russian], 156 pp., Nauka, Moscow, 1982.

39. Arkhipov, S.A., and V.S. Volkova, *Pleistocene geological history, landscapes, and climates of West Siberia* [in Russian], 105 pp., UIGGM SB RAS, Novosibirsk, 1994.

40. Khotinsky, N.A., *The Holocene of Northern Eurasia* [in Russian], 200 pp., Nauka, Moscow, 1997.

41. Mann, D.H., and D.M. Peteet, Extent and Timing of the Last Glacial maximum in Southwestern Alaska, *Quatern. Res.*, **42**, 136–148, 1994.

42. Whitlock, C., and P. Bartlein, Vegetation and climate change in northwest America during the past 125 kyr, *Nature*, **388**, 57–61, 1997.

43. Reasoner, M.A., and U.M. Huber, Postglacial palaeoenvironments of the upper Bow Valley, Banff National Park, Alberta, Canada, *Quatern. Sci. Rev.*, **18**, 475–492, 1999.

44. Andreev, A.A., P.E. Tarasov, F.A. Romanenko, and L.D. Sulerzhitsky, The Younger Dryas pollen records from Sverdrup Island (Kara Sea), *Quatern. Intern.*, **41/42**, 235–247, 1998.

45. Andreev, A.A., P.E. Tarasov, F.A. Romanenko, L.D. Sulerzhitsky, and K.I. Terekhov, The Late Pleistocene and Holocene vegetation evolution on the western coast of Baidaratskaya Bay, *Stratigrafiya i Geologicheskie Korrelyatsii*, **5**, 135–139, 1997.

46. Krainov, M.A., and V.A. Kravchinsky, Rock-magnetic study of deep-water Baikal sediments: implication

to Neogene-Quaternary climate in Asia, *International workshop for the Baikal & Hovsgol drilling project in Ulanbaatar: Abstracts of the Workshop, 2001, October 4–7*. Ulanbaatar, p. 36, 2001.

47. Prokopenko, A.A., E.B. Karabanov, D.F. Williams, M.I. Kuz'min, G.K. Khursevich, and A.N. Gvozdkov, The link between tectonic and paleoclimatic events at 2.8–2.5 Ma BP in the Lake Baikal region, *Quatern. Intern.*, **80–81**, 37–46, 2001.

48. Khursevich, G.K., E.B. Karabanov, A.A. Prokopenko, et al., New fossil species of Cyclotella (Bacillariophyta) from Upper Cenozoic deposits of Lake Baikal, Siberia and their stratigraphic significance. International Project on Paleolimnology and Late Cenozoic Climate, *IPPCCE Newsletter*, 12, 62–76, 1999.

49. Karabanov, E.B., *Pleistocene—Holocene paleoclimate record of Lake Baikal, PhD Thesis*, 184 pp., University of South Carolina, Columbia, SC, USA, 1997.

50. Shackleton, N.J., A. Berger, and W.R. Peltier, An alternative astronomical calibration of the lower Pleistocene timescale based on ODP site 677, Transition of Royal Society, Edinburg, *Earth Sci.*, **81**, 251–261, 1990.

51. Bezrukova, E.V., Yu.A. Bogdanov, D.F. Williams, L.Z. Granina, M.A. Grachev, N.V. Ignatova, E.B. Karabanov, V.M. Kuptsov, A.B. Kurylev, P.P. Letunova, E.V. Likhoshway, G.P. Chernyaeva, M.K. Shimaraeva, and A.O. Yakushin, Deep changes of the North Baikal ecosystem in the Holocene, *Doklady AN SSSR*, **321**, 5, 1032–1036, 1991.

52. Prokopenko, A.A., E.B. Karabanov, D.F. Williams, M.I. Kuz'min, N.J. Shackleton, S.J. Crowhurst, J.A. Peck, A.N. Gvozdkov, and J.W. King, Biogenic silica record of the Lake Baikal: response to the climatic forcing during the Brunhes, *Quatern. Res.*, **55**, 123–132, 2001.

53. Arkhipov, S.A., V.S. Zykina, A.A. Krukover, Z.N. Gnibidenko, and V.N. Shelkoplyas, Stratigraphy and paleomagnetism of glacial and loess-soil deposits on the West-Siberian Plain, *Geologiya i Geofizika (Russian Geology and Geophysics)*, **38**, 6, 1027–1048(1065–1085), 1997.

54. Karabanov, E.B., A.A. Prokopenko, D.F. Williams, A.N. Gvozdkov, and E.V. Kerber, Glacial and interglacial periods of Siberia: the Lake Baikal paleoclimatic record and correlation with West Siberian stratigraphic scheme (the Brunhes Chron), *Geologiya i Geofizika (Russian Geology and Geophysics)*, **42**, 1, 48–63(41–54), 2001.

55. Kuz'min, M.I., E.B. Karabanov, A.A. Prokopenko, D.F. Williams, A.N. Gvosdkov, and V.F. Geletiy, Climatic events in Siberia during upper Brunhes according to the Lake Baikal sedimentary record, *Berliner Geowiss. Abh.*, Berlin, **E30**, 315–323, 1999.

56. Laskar, J., F. Joutel, and F. Boudin. Orbital, precessional and insolation quantities for the Earth from –20 Myr to +10 Myr, *Astronomy and Astrophysics*, **270**, 522–533, 1993.

57. Tzedakis, P.C. Long-term populations in northwest Greece through multiple Quaternary climatic cycles, *Nature*, **364**, 473–440, 1993.

58. Arkhipov, S.A., Pleistocene chronostratigraphy of northern Siberia, *Geologiya i Geofizika (Soviet Geology and Geophysics)*, **30**, 6, 13–22(11–20), 1989.

59. Kuz'min, M.I., V.V. Yarmoluyk, and E.V. Karabanov, Paleoclimate records from the Lake Baikal, lava formations of the South-Baikal volcanic area, in *A long continental record from Baikal*, ed. Kenij Kashiwaya, 23–42, Springer Verlag, Tokyo, 2003.

60. Levina, O.V., V.A. Bychinskii, O.A. Proidakova, O.Yu. Astrakhantseva, and L.A. Pavlova, Chemical composition and thermodynamic properties of diatom frustules as applied to the dissolution and sedimentation of biogenic silica in Lake Baikal, *Geologiya i Geofizika (Russian Geology and Geophysics)*, **42**, 2, 319–328(307–316), 2001.

61. Flower, R.J., A.W. Mackay, N.L. Rose, J.L. Boyle, J.A. Dearling, P.G. Appleby, A.E. Kuz'mina, and L.Z. Granina, Sedimentary records of recent environmental change in Lake Baikal, Siberia, *The Holocene*, **5**, 323–327, 1995.

62. Belova, S.A., *Late Cenozoic vegetation and climate in southern East Siberia* [in Russian], 158 pp., Nauka, Novosibirsk, 1985.

63. Savina, L.N., The evolution trend of coastal landscapes around Lake Baikal, from paleogeographic data, in *Late Cenozoic history of lakes in the USSSR* [in Russian], eds. V.A. Belova and B.F. Lut, 42–52, Nauka, Novosibirsk, 1982.

64. Bezrukova, E.V., V.D. Matz, P.P. Letunova, T. Nakamura, and Sh. Fuji, Holocene peatbogs in Prebaikalia as an object of paleoclimatic reconstructions, *Geologiya i Geofizika (Russian Geology and Geophysics)*, **37**, 12, 78–92(76–89), 1996.

65. Bezrukova, E.V., H. Takakhara, S.K. Krivonogov, K.E. Vershinin, H. Mioyshi, T. Nakamura, A.A. Abzaeva, Y. Morita, K. Kawamuro, T. Shinomiya, C.M. Krapivina, The Late Quaternary and Holocene history of the southeastern coast of Lake Baikal, from well log data, Dulikha well, in *Reconstructions of Holocene*

and Pleistocene environments in Siberia [in Russian], eds. E.A. Vaganov, A.P. Derevyanko, and V.S. Zykin, 36–48, IAE SB RAS, Novosibirsk, 2000.

66. Vipper, P.B., N.V. Dorofeyuk, A. Lijva, and E.P. Metel'tseva, Holocene paleogeography of Central Mongolia, *Izv. AN SSSR, Ser. Biol.*, 30, 74–82, 1981.

67. Pevzner, L.A., O.G. Badalov, O.A. Esipko, and E.V. Neronova, Geophysical studies in deepwater drill holes in Lake Baikal, *Razvedka i Okhrana Nedr*, **11**, 8–14, 1999.

68. BDP Members, The new BDP 98 600-m drill core from Lake Baikal: a key Late Cenozoic sedimentary section in continental Asia, *Quatern. Intern.*, **80–81**, 19–36, 2001.

69. Logachev, N.A. (ed.), *Uplands of Pribaikalia and Transbaikalia.* [in Russian], 357 pp., Nauka, Moscow, 1974.

70. Matz, V.D. The structure and development of the Baikal rift depression, *Earth. Sci. Rev.*, **34**, 81–118, 1993.

71. Bukharov, A.A., *Lake Baikal in figures. Baikal Museum* [in Russian], 71 pp., ISC SB RAS, Irkutsk, 2001.

72. Back S., M. DeBatist, P. Kirillov, M. Strecker, and P. Vanhauwaert, The Frolikha fan: a large Pleistocene glaciolacustrine outwash fan in northern lake Baikal, Siberia, *J. Sedim. Res.*, **68**, 841–849, 1998.

73. Osipov, E.Yu., M.A. Grachev, V.D. Matz, S. Brietenbach, and O.M. Khlystov, Paleoglaciological reconstruction of the Last Glacial maximum in the northern part of the Barguzin Ridge, North-East of Lake Baikal, *PAGES Meeting on High Latitude Paleoenvironments, Moscow, May 16–17, 2002. Program and Abstracts.* Moscow, p. 39, 2002.